ISTANBUL TECHNICAL UNIVERSITY ★ GRADUATE SCHOOL OF SCIENCE ENGINEERING AND TECHNOLOGY

SYNTHESIS OF PROTON EXCHANGE MEMBRANE BY ATRP AND INIFERTER METHODS

M.Sc. THESIS

Cüneyt Erdinç TAŞ

Department of Polymer Science and Technology

Polymer Science and Technology Programme

Thesis Advisor: Prof. Dr. Metin H. ACAR

JANUARY 2013

ISTANBUL TECHNICAL UNIVERSITY ★ GRADUATE SCHOOL OF SCIENCE ENGINEERING AND TECHNOLOGY

SYNTHESIS OF PROTON EXCHANGE MEMBRANE BY ATRP AND INIFERTER METHODS

M.Sc. THESIS

Cüneyt Erdinç TAŞ

Department of Polymer Science and Technology

Polymer Science and Technology Programme

Thesis Advisor: Prof. Dr. Metin H. ACAR

JANUARY 2013

İSTANBUL TEKNİK ÜNİVERSİTESİ ★ FEN BİLİMLERİ ENSTİTÜSÜ

ATRP VE İNİFERTER YOLU İLE İYONİK İLETKENLİĞE SAHİP POLİMER SENTEZİ

YÜKSEK LİSANS TEZİ

Cüneyt Erdinç TAŞ
(515101004)

Polimer Bilim ve Teknolojileri

Polimer Bilim ve Teknolojileri Programı

Tez Danışmanı: Prof. Dr. Metin H. ACAR

OCAK 2013

Cüneyt Erdinç TAŞ, a **M.Sc.** student of ITU **Institute of Science and Technology/ Graduate School of Istanbul Technical University** student ID 515101004, successfully defended the **thesis** entitled "**Sythesis of Proton Exchange Mambrane by ATRP and Iniferter methods**", which he prepared after fulfilling the requirements specified in the associated legislations, before the jury whose signatures are below.

Thesis Advisor :	**Prof. Dr. Metin H. ACAR** İstanbul Technical University	.....
Jury Members :	**Prof.Dr. Name SURNAME** İstanbul Technical University	.....
	Prof. Dr. Name SURNAME Yıldız Technical University	.....

Date of Submission : 17 December 2012
Date of Defense : 21 January 2013

To my parents,

FOREWORD

This master project was carried out at Istanbul Technical University, Chemistry Department of Science & Letters Faculty, Pol-Merg Laboratory under the teaching supervisor of Prof. Metin H. ACAR, under support of Istanbul Technical University Institute of Science and Technology.

I would like express my deep pride, regards and thanks to my supervisor Prof. Metin H. ACAR for his sincere supervision, advice, and guidance of this study. He supported me during thesis and guided to open my mind for research to look for different views. Through his wealth of knowledge, direction and leadership I have been able to expand my knowledge in many areas of polymer science. It was a great pleasure for me to work with him.

I would like to acknowledge Dr. Sebnem INCEOGLU. I would like to thank to Atilay TUZER, Damla GULFIDAN, Ari Sant BILAL, Mehmet BASDAL, Buket ALKAN, Eren ELIK, Merve BAYRAKTAR, Gizem GUDEN and Deniz KOPAN for their help, support and friendship. Many thank to Giray Ersozoglulari for Impedance measurements.

I would like to thank to neighbour laboratories and my special friends, Ipek OSKEN and Dr. Aydan DAG, for their advice about measurements and their great friendship, and Hakan BILDIRIR for their friendship and advice.

I would like to thank to the other neighbour laboratory and my friends Dr. Eda GUNGOR, Dr. Hakan DURMAZ.

I also want to thank my parents and brother for their patience and supports during this thesis.

At the end, I would like to thank everybody to who helped me to walk this way.

December 2012

Cüneyt Erdinç TAŞ
Chemist

TABLE OF CONTENTS

Page

FOREWORD ..... **ix**
TABLE OF CONTENTS ..... **xi**
ABBREVIATIONS ..... **xiii**
LIST OF TABLE ..... **xv**
LIST OF FIGURES ..... **xvii**
SUMMARY ..... x**ix**
ÖZET ..... **xxi**
1. INTRODUCTION **1**
2. THEORETICAL PART **7**
2.1 Fuel Cells 7
2.1.1 Introduction and historical development 8
2.1.2 Fuel cell systems 9
2.1.3 Types of fuel cells 10
2.1.4 Applications of fuel cells 11
2.2 Polymer Electrolyte Membrane Fuel Cell (PEMFC) 12
2.2.1 Introduction of PEMFC 12
2.2.2 Commercial proton exchange membrane fuel cell 13
2.2.2.1 General 13
2.2.2.2 Nafion 13
2.2.3 Proton conductivity 14
2.2.4 Water management 15
2.3 Living Polymerization 16
2.4 Controlled / Living Radical Polymerizations 17
2.4.1 Atom transfer radical polymerization (ATRP) 18
2.4.1.1 About ATRP 18
2.4.1.2 Kinetics and mechanism of ATRP 19
2.4.2 Components of ATRP 22
2.4.2.1 Monomers 23
2.4.2.2 Initiators 23
2.4.2.3 Catalyst and transition metals 25
2.4.2.4 Ligands 25
2.4.2.5 Solvents 26
2.4.2.6 Temperature and reaction time 26
2.4.3 Iniferters 26
2.4.4 Reversible addition–fragmentation chain transfer process (RAFT) 29
2.5 Graft copolymer 31
2.5.1 Grafting through 32
2.5.2 Grafting from 34
2.5.3 Grafting onto 34
2.6 Photopolymerization 35

2.7 Poly(vinyl chloride) (PVC) 36
3. EXPERIMENTAL PART 41
3.1 Chemicals 41
3.2 Synthesis of P(VC-*g*-AMPS) Graft Copolymer by ATRP 42
3.3 Synthesis of PVC-DDC (Diethyl dithiocarbomate) 43
3.4 Synthesis of P(VC-*g*-AMPS) Graft Copolymer by Iniferter Method 43
3.5 Characterization Methods 43
3.5.1 Infrared spectrometer (FT-IR) 43
3.5.2 UV-Visible spectrofotometer 44
3.5.3 Gel permeation chramatography 44
3.5.4 Differential scanning calorimetry 45
3.5.5 Electrochemical impedance spectroscopy 45
3.5.6 Nuclear magnetic resonance spectroscopy 46
3.5.7 Thermal gravimetric analysis 47
4. RESULTS AND DISCUSSION 49
4.1 PVC-Based Garft Copolymer 49
4.1.1 P(VC-*g*-AMPS) graft copolymer via ATRP 50
4.1.2 Synthesis of PVC-DDC 58
4.1.3 P(VC-*g*-AMPS) graft copolymer via iniferter method 60
5. CONCLUSION 67
REFERENCES 69
CURRICULUM VITAE 73

ABBREVIATIONS

ATRP	: Atom transfer radical polymerization
CRP	: Controlled radical polymerization
DDC	: *N*,*N*-Diethyl dithiocarbomate
PVC	: Poly(vinyl chloride)
AMPS	: 2-Acrylamido-2-methylpropane sulfonic acid
RAFT	: Reversible Addition Fragmentation Chain Transfer
NMP	: Nitroxide mediated polymerization
MA	: Methyl acrylate
MMA	: Methyl metacrylate
C/LRP	: Controlled / living radical polymerization
AIBN	: Azobis(isobutyronitrile)
BA	: Butyl acrylate
EHA	: Ethyl hexyl acrylate
Me_6TREN	: tris(2-dimethylaminoethyl)amine
PMDETA	: N,N,N',N'',N‴-pentamethyldiethylenetriamine
DLS	: Dynamic light scattering
EF-TEM	: Energy filtered-transmission electron microscopy
PECH	: Poly(epichlorohydrin)
PEM	: Polymer electrolyte membrane
MeOH	: Metahanol
PEMFC	: Polymer electrolyte membrane fuel cell
EIS	: Electrochemical impedance spectroscopy
PAFC	: Phosphoric acid fuel cell
RI	: Refractive index
PS	: Polystyrene
PDI	: Polydispersity index
DMSO	: Dimethyl sulfoxide
MEK	: Methyl ethyl ketone
DMF	: Dimethyl formamide
THF	: Tetrahydrofuran
NMP	: N-Methylpyrrolidone
NMR	: Nuclear magnetic resonance
FT-IR	: Fourier transform infrared spectroscopy
TGA	: Thermogravimetric analysis
DSC	: Differential scanning calorimeter
T_g	: Glass transition temperature

LIST OF TABLE

Page

Table 2.1 : Graft copolymerization characteristics of BA and EHA from PVC 37
Table 3.1 : Chemical structures of PVC and Nafion®-117 41
Table 4.1 : Previous experiments 49
Table 4.2 : T_g values of pure PVC and and P(VC-*g*-AMPS) at 5,24 and 48 hours .. 54
Table 4.3 : M_n and PDI values of the samples 55
Table 4.4 : M_n, PDI and R_h value of the samples by GPC-TD 56
Table 4.5 : T_g values of PVC, PVC-DDC and P(VC-*g*-AMPS) 62
Table 4.6 : DDC group content of PVC-DDC 63

LIST OF FIGURES

Page

Figure 2.1 : Schematic of PEM fuel cell. 7
Figure 2.2 : Grove's fuel cell experiment. 9
Figure 2.3 : Schematic views of a PEM fuel cell and a seven-layered MEA. 10
Figure 2.4 : Chemical structure of Nafion® (DuPont). 14
Figure 2.5 : Water management. 15
Figure 2.6 : Mechanism for ATRP 20
Figure 2.7 : Kinetic plot and conversion vs. time plot for ATRP. 21
Figure 2.8 : Some of the monomers used in ATRP. 23
Figure 2.9 : ATRP initators; halogenated alkanes and benzylic halides. 24
Figure 2.10 : ATRP initators; α-bromoesters. 24
Figure 2.11 : ATRP initators; sulfonyl chlorides. 24
Figure 2.12 : Some of the ligands using ATRP. 26
Figure 2.13 : Mechanism of iniferters. 27
Figure 2.14 : A-A or A-B type of iniferters 28
Figure 2.15 : B-B type of iniferters. 28
Figure 2.16 : Main classes of RAFT agents. 29
Figure 2.17 : Proposed general mechanism of RAFT polymerization. 30
Figure 2.18 : Strategies for the synthesis of graft copolymer: (a) ''grafting onto'', (b) ''grafting from'', and (c) ''grafting through''. 32
Figure 2.19 : Grafting through via ATRP. 32
Figure 2.20 : Homogeneous distribution of graft (a) and heterogeneous distribution of graft (b). 33
Figure 2.21 : Grafting from method. 34
Figure 2.22 : Grafting of acrylate monomers from labile chlorines of PVC. 37
Figure 2.23 : Polymerization of AMPS via ATRP. 38
Figure 2.24 : Synthesis of Poly(epichlorohydrin) (PECH) with pendent N,N-diethyl dithiocarbamate groups (PECH-DDC). 39
Figure 2.25 : Sythesis of PECH-*g*-PMMA via iniferter polymerization. 39
Figure 3.1 : 2-Acrylamido-2-methylpropan sulfonic acid (AMPS). 42
Figure 3.2 : Sodium diethyldithiocarbomate used as iniferter precursor. 42
Figure 3.3 : Gel permeation chromotography. 44
Figure 3.4 : Triple detector GPC. 45
Figure 3.5 : Differential scanning calorimetry (Q1000). 45
Figure 3.6 : General diagram of electrochemical impedance spectroscopy. 46
Figure 3.7 : Agilent VNMRS500 NMR insturment. 47
Figure 3.8 : TA-Q50 TGA instrument. 47
Figure 4.1 : Synthesis of P(VC-*g*-AMPS) graft copolymer via ATRP. 50
Figure 4.2 : UV-Visible spectra of P(VC-*g*-AMPS). 51
Figure 4.3 : IR spectrum of AMPS monomer, PVC and the samples of P(VC-*g*-AMPS) at 5, 24 and 48 hours 51

Figure 4.4 : IR spectrum of PVC and P(VC-*g*-AMPS) at 5, 24 and 48 hours. 52
Figure 4.5 : DSC curves of P(VC-*g*-AMPS) at 5,24 and 48 hours (first heating cycle). 53
Figure 4.6 : DSC curves of PVC and P(VC-*g*-AMPS) at 5,24 and 48 hours (second heating cycle). 53
Figure 4.7 : The conventional GPC measurements of PVC and P(VC-*g*-AMPS) at 5,24 and 48 hours 54
Figure 4.8 : Triple detector GPC measurements of PVC and P(VC-*g*-AMPS) at 5,24 and 48 hours. 56
Figure 4.9 : Nyquist graph of EIS measurements. 57
Figure 4.10 : Magnetude graph of EIS measurements. 57
Figure 4.11 : TGA result of P(VC-*g*-AMPS) via ATRP. 58
Figure 4.12 : The synthesis route of PVC-DDC. 58
Figure 4.13 : IR spectrum of PVC and PVC-DDC. 59
Figure 4.14 : UV spectrum of PVC and PVC-DDC. 59
Figure 4.15 : ^{1}H NMR spectrum of PVC-DDC. 60
Figure 4.16 : Synthesis of P(VC-*g*-AMPS) by iniferter. 60
Figure 4.17 : FT-IR result of P(VC-*g*-AMPS) by iniferter. 61
Figure 4.18 : DSC result of P(VC-*g*-AMPS) by iniferter. 61
Figure 4.19 : ^{1}H NMR of P(VC-*g*-AMPS) by iniferter. 62
Figure 4.20 : UV-Visible spectrophotometer results of PVC-DDC_2 and P(VC-*g*-AMPS) graft copolymer via iniferter method. 63
Figure 4.21 : TGA result of P(VC-*g*-AMPS) graft copolymer via iniferter. 64
Figure 4.22 : DMF GPC results of PVC and P(VC-*g*-AMPS) by ATRP method. 64
Figure 4.23 : DMF GPC results of PVC and P(VC-*g*-AMPS) by iniferter. 65
Figure 4.24 : Nyquist graph of EIS measurements for ATRP and iniferter method. 65

SYNTHESIS OF PROTON EXCHANGE MEMBRANE BY ATRP AND INIFERTER METHODS

SUMMARY

The proton exchange membrane fuel cell (PEMFC) uses a water-based, acidic polymer membrane as its electrolyte, with platinum-based electrodes. PEMFC cells operate at relatively low temperatures (below 100 degrees Celsius) and can tailor electrical output to meet dynamic power requirements. Due to the relatively low temperatures and the use of precious metal-based electrodes, these cells must operate on pure hydrogen. PEMFC cells are currently the leading technology for light duty vehicles and materials handling vehicles, and to a lesser extent for stationary and other applications. The PEMFC fuel cell is also sometimes called a polymer electrolyte membrane fuel cell (also PEMFC).

Fuel cells have various advantages compared to conventional power sources, such as internal combustion engines or batteries. Although some of the fuel cells' attributes are only valid for some applications, most advantages are more general.

Fuel cells have a higher efficiency than diesel or gas engines. Fuel cells can eliminate pollution caused by burning fossil fuels; for hydrogen fuelled fuel cells, the only by-product at point of use is water. If the hydrogen comes from the electrolysis of water driven by renewable energy, then using fuel cells eliminates greenhouse gases over the whole cycle. Fuel cells do not need conventional fuels such as oil or gas and can therefore reduce economic dependence on oil producing countries, creating greater energy security for the user nation. Since hydrogen can be produced anywhere where there is water and a source of power, generation of fuel can be distributed and does not have to be grid-dependent. The use of stationary fuel cells to generate power at the point of use allows for a decentralised power grid that is potentially more stable. Operating times are much longer than with batteries, since doubling the operating time needs only doubling the amount of fuel and not the doubling of the capacity of the unit itself.

The main goal of this study is to design a polymeriz material and to investigated thermal properties and ion conductivity of this material. In this study, PVC based graft copolymer was synthesized and AMPS as sulfonic acid groups containing monomer were used. Two different polymerization methods, ATRP and iniferter polymerization method, were used in order to synthesis of PVC based graft copolymers. These synthesises were characterizated by using FT-IR, UV-Visible spectrophotometer, DSC, ^{1}H NMR, conventional and triple detector systems GPC.

Proton conducting properties were investigated via Electrochemical Impedance Spectroscopy (EIS).

ATRP VE İNİFERTER YOLU İLE İYONİK İLETKENLİĞİNE SAHİP POLİMER SENTEZİ

ÖZET

1950'li yıllarda General Electric tarafından bulunan PEM teknolojisi, o yıllarda ilk defa NASA tarafından Gemini uzay aracında güç ünitesi olarak kullanılmıştır. Günümüzde PEM yakıt pilleri otomotiv sektöründe içten yanmalı motorlara alternatif olarak geliştirilmekte ve kullanılmaktadır.

Proton değişim membran yakıt hücreleri, özellikle yüksek performanslı polimerlerin bulunmasından sonra; uzay çalışmalarında ve özel askeri sistemlerde uygulanmak amacıyla geliştirilmiştir. Günümüz teknolojisi ile hertürlü güç gereksiniminin olduğu yerlerde kullanılmakta ve yaygınlaşnmaktadır. Proton değişim membran yakıt hücreleri düşük çalışma sıcaklığında yüksek verim elde edilmesi, sessiz çalışması ve saf suyun dışında herhangi bir atık ortaya çıkarmamasından dolayı en çok ilgi çeken yakıt hücresi türüdür.

PEM yakıt hücrelerinin temel bileşeni anot ve katot olmak üzere iki tane elektrot içerir. Bunlar birbirlerinden polimer membran elektrolit ile ayrılmışlardır. Her iki elektrot bir kenarlarından ince platin katalizör tabakası ile örtülmüştür. Yakıt olarak kullanılan hidrojen yakıt hücresinin anot kenarından beslenir. Anotta platin katalizör varlığında serbest elektronlar ve protonlara ayrışır. Serbest elektronlar dış çevrimde kullanılırlar ve elektrik akımını oluştururlar. Protonlar polimer membran elektroliti geçerek katota doğru hareket ederler, katotta havadan gelen oksijen dış çevrimden gelen elektronlar ve protonlar saf su ve ısı oluşturmak üzere birleşirler. Tek bir yakıt hücresi yaklaşık 0,6 volt güç üretir, istenilen elektriksel güç miktarını karşılamak için yakıt hücreleri birleştirilirler**.**

PEM yakıt pillerinde, elektrotlar karbon yapılı olup, kullanılan elektrolit ise ince bir polimer membrandır. En çok kullanılan membran, poli[perflorosülfonik] asit veya Nafyon'dur. Bu ince polimer tabakadan protonlar kolayca diğer tarafa geçebilirken, elektronların geçişi mümkün değildir. Hidrojen anot üzerine akarken, elektrot yüzeyinde hidrojen iyonlarına (proton) ve elektronlarına ayrılır. Oluşan hidrojen iyonları ince membrandan katoda doğru ilerlerken, geçişi engellenen elektrotlar dış devreden geçerek güç oluştururlar.
Havadan sağlanan oksijen katot üzerinde hidrojen iyonları ve dış devreden gelen elektronlar ile birleşerek suyun oluşmasını sağlar. PEM yakıt pili elektrotları üzerinde gerçekleşen reaksiyonlar aşağıdaki gibidir;

$H_2\ (g) \rightarrow 2H^+ + 2e^-$ anot tepkimesi

$2H^+ + 2e^- + 1/2O_2 \rightarrow H_2O$ katot tepkimesi

PEM yakıt pilleri 80°C sıcaklıkta çalıştıklarından ve bu sıcaklık, gerçekleşen elektrokimyasal reaksiyonlar için düşük olduğundan elektrotlar ince platin tabakaları ile desteklenmektedirler. PEM yakıt pillerinin otomotiv sektöründe kullanımını sağlayan önemli avantajları vardır. Bu avantajlar; küçük boyutta uygulanabilirlikleri, düşük sıcaklıklarda çalışmalarına rağmen bu sıcaklıklardan kolayca yüksek güç üretimine geçebilmeleridir. Bunların yanında, yüksek verimde çalışmaları, % 40-50 seviyesinde maksimum teorik voltaj üretebilmeleri ve güç ihtiyacındaki değişikliklere hızlı cevap verebilmeleri de PEM yakıt pillerini tercih edilir konuma getirmektedir.

Proton değişim membran yakıt hücrelerinin en önemli elemanı proton iletim özelliğine sahip polimerik membrandır. Yakıt hücreleriyle ilgili yapılan çalışmaların başında polimerik membranların geliştirilmesi ile ilgili olan çalışmalar yer almaktadır. Günümüzde ticari olarak kullanılan membranların çeşitliliğinin az ve fiyatlarının yüksek olmasından dolayı alternatif membranların geliştirilmesi ile ilgili çalışmalar oldukça hızlanmıştır. Proton değişim membran yakıt hücrelerinde kullanılan membranların;

- · Proton geçirgen özellikte olması,
- · Su, yakıt (hidrojen veya metanol), oksijen ve havadaki diğer gazları geçirmemesi
- · Mekanik dayanımının yüksek olması,
- · Uzun süreli kullanımda ısıl ve kimyasal direnci yüksek,
- · Teknolojik olarak yaygın bir şekilde kullanılabilmesi için emniyetli ve ucuz olması gerekmektedir.

Proton değişim yakıt hücrelerinde kullanılan membranların yüksek verimle çalışabilmeleri için su ile tamamen doyurulmuş olmaları gerekmektedir. Yapılan çalışmalarda membranın tam doygun olduğu zaman yüksek iyonik iletkenliğe ulaşıldığı görülmektedir.

Membran çok ince bir yapıya sahip olmasına rağmen çok etkili bir gaz ayrıştırıcıdır. Hidrojen yakıtı, oksidant havadan ayırıp ayrı tutabilme kabiliyetine sahip olup bu özellik yakıt pilinin çalışma verimine esas oluşturmaktadır. Membran iyonik iletken olmasına rağmen elektronları geçirmez. Organik doğası gereği elektronik yalıtkandır. Bu durum ise yakıt pilinin çalışmasının diğer bir esasıdır. Plakadan geçmeyen elektronlar, harici bir devre yardımıyla hücrenin diğer tarafına (katot) alınır ev devrelerini tamamlarlar.

Bu çalışmada ana zincir olarak PVC kullanılıp, bu polimere sülfon grubu içeren AMPS monomeri aşı kopolimerizasyonu ilebağlanmıştır. P(VC-*g*-AMPS) aşı kopolimerinin sentezlenmesi için iki farklı polimerizasyon çeşidi kullanılmıştır. Bunlar ATRP ve iniferter polimerizasyon metotlarıdır.

ATRP çok yönlü kontrollü radikal polimerizasyon metotlarından biridir. Bir ATRP sistemi; başlatıcı, metal halojenür, ligand ve monomerden oluşmaktadır. Düşük oksidasyon basamağına sahip metal kompleksi (M_t^n compleks/Ligand), radikal ve daha yüksek oksidasyon basamağına sahip metal kompleksi (X-M_t^{n+1}/Ligand) üretmek üzere alkil halojenür (R-X) ile reaksiyona girer. Oluşan radikal monomere eklenir ve böylece polimer zincirinde büyüme gerçekleşir. Reaksiyonun ilerleme aşaması halojenürün koparılması sonucu oluşan serbest radikal üzerinden ilerler. Serbest radikal metalden halojenürü tekrar koparır ve aktif olmayan ürün oluşur. Bu işlemler oldukça hızlıdır ve reaksiyonda denge aktif olmayan ürün oluşumu yönündedir. Aktivasyon ve deaktivasyon hız sabitlerinin oranına bağlı olarak bir süre

sonra büyüyen zincir yine aktif hale gelir ve büyümeye devam eder. Bu basamaklar tekrarlanarak kontrollü zincir büyümesi sağlanmış olur. Sonlanma tamamen önlenemez, ancak sonlanan zincirlerin oranı büyüyen zincirlerle karşılaştırıldığında sonlanan zincirlerin sayısı oldukça küçüktür.

ATRP reaksiyonu ortamdaki monomer bitene kadar ya da reaksiyon koşulları bozulana kadar devam eden bir yaşayan polimerleşme tekniğidir. İstenilen ağırlıkta polimer elde edene kadar reaksiyon devam edebilir ve reaksiyonu durdurmak için dışarıdan müdahale gerekmektedir.

Bu çalışmanın ATRP basamağında, PVC makro başlatıcı olarak kullanılmış ve PVC ye ait klor gruplarından reaksiyon gerçekleşmiştir.

Diğer yöntem olan iniferter polimerizasyonu ise bir iniferter grubun ışık veya ısı ile radikal üretmesi ve monomerin başlatıcı radikali ile kontrollü mekanizmayı sağlayan sonlandırıcı radikal grubunun arasına dolması ile gerçekleşir. Bu kontrollü radikal polimerizaston tipi ilk olarak 1982 yılında Otsu ve Yoshida tarafından gerçekleştirilmiştir. Monofonksiyonel fotoiniferter BDC (Benzil-N,N-dietilditiyokarbomat) ve bifonksiyonel fotoiniferter XDC (Ksilen bis N,N-dietilditiyokarbomat) bazı monomerlerin yaşayan polimerizasyonları için kullanılmıştır [49]. Bu çalışmada iniferter grup olarak, sodyum dietilditiyokarbomat kullanılmıştır. Makrobaşlatıcı olarak önce PVC ile sodyum dietil ditiyokarbomat reaksiyona sokulmuş ve PVC-DDC makrobaşlatıcısı sentezlenmiştir. Ardından ışık ile PVC üzerinde bulunan DDC gruplarından iniferter polimerizasyonu gerçekleştirilmiş ve istenen P(VC-*g*-AMPS) aşı kopolimeri elde edilmiştir.

İki farklı metotla sentezlenen P(VC-*g*-AMPS) aşı kopolimeri FT-IR, UV-Visible, DSC, ^{1}H NMR, klasik GPC ve üçlü dedektör GPC sistemleri ile karakterize edilmiştir.

Sentezlenen maddelerin iyon iletkenlikleri Elektrokimyasal Empedans Spektrometresi ile incelenmiştir.

1. INTRODUCTION

Energy consumption, which is heavily dependent on burning fossil fuels, plays an important role in our daily life. The increasing threat by the fast depletion of the resources of petroleum, coal and natural gas, and, in turn, the green house effect by burning fossil fuels, forces people to seek regenerative energy sources, such as solar, wind, geothermal and hydroelectric energies. The greenhouse effect occurs due to the excess emission of carbon dioxide and it has become a major concern, and non-polluting fuels and a clean environment are clear targets. Fossil fuel consumption is the major causation to the increasing concentration of carbon dioxide (CO_2) in the atmosphere, a key cause of global warming. Global warming reduces agricultural production and causes other biological and social problems. For example, The United States, with less than 4% of the world population, emits 22% of the CO_2 from burning fossil fuels, more than any other nation. Reducing fossil fuel consumption may slow the rate of global warming. An alternative way to save valuable natural resources and solve the environmental problem is to develop cleaner and more efficient energy conversion devices [1-2].

Renewable energy supplies are of ever increasing environmental and economic importance in all countries. A wide range of renewable energy Technologies are established commercially and recognised as growth industries by most governments. Reliable energy supply is essential in all economies for lighting, heating, communications, computers, industrial equipment, transport, etc. World energy use increased more than tenfold over the 20th century, predominantly from fossil fuels (i.e. coal, oil and gas) and with the addition of electricity from nuclear power. In the 21st century, further increases in world energy consumption can be expected, much for rising industrialisation and demand in previously less developed countries, aggravated by gross inefficiencies in all countries. Without new supplies such growth cannot be maintained. So an obvious conclusion to overcome such constraints is to increase renewable energy supplies. Energy is useful only if available when and

where it is wanted. Carrying energy to where it is wanted is called distribution or transmission; keeping it available until when it is wanted is called storage [3].

Hydrogen is the simplest element. An atom of hydrogen consists of only one proton and one electron. It's also the most plentiful element in the universe. Despite its simplicity and abundance, hydrogen doesn't occur naturally as a gas on the Earth - it's always combined with other elements. Water, for example, is a combination of hydrogen and oxygen (H_2O).

Hydrogen is also found in many organic compounds, notably the *hydrocarbons* that make up many of our fuels, such as gasoline, natural gas, methanol, and propane. Hydrogen can be separated from hydrocarbons through the application of heat - a process known as *reforming*. Currently, most hydrogen is made this way from natural gas. An electrical current can also be used to separate water into its components of oxygen and hydrogen. This process is known as*electrolysis*. Some algae and bacteria, using sunlight as their energy source, even give off hydrogen under certain conditions.

Hydrogen is high in energy, yet an engine that burns pure hydrogen produces almost no pollution. NASA has used liquid hydrogen since the 1970s to propel the space shuttle and other rockets into orbit. Hydrogen fuel cells power the shuttle's electrical systems, producing a clean byproduct - pure water, which the crew drinks.

A fuel cell combines hydrogen and oxygen to produce electricity, heat, and water. Fuel cells are often compared to batteries. Both convert the energy produced by a chemical reaction into usable electric power. However, the fuel cell will produce electricity as long as fuel (hydrogen) is supplied, never losing its charge.

Fuel cells are a promising technology for use as a source of heat and electricity for buildings, and as an electrical power source for electric motors propelling vehicles. Fuel cells operate best on pure hydrogen. But fuels like natural gas, methanol, or even gasoline can be reformed to produce the hydrogen required for fuel cells. Some fuel cells even can be fueled directly with methanol, without using a reformer.

In the future, hydrogen could also join electricity as an important energy carrier. An energy carrier moves and delivers energy in a usable form to consumers. Renewable energy sources, like the sun and wind, can't produce energy all the time. But they could, for example, produce electric energy and hydrogen, which can be stored until

it's needed. Hydrogen can also be transported (like electricity) to locations where it is needed [4].

The power and energy efficiency of a fuel cell is highly dependent on the thermodynamics, electrode kinetics, reactant mass transfer, as well as materials and components for assembling the fuel cell. These factors have been addressed throughout the fuel cell history, and are now still the major challenges for fuel cell research and development. Two key issues limiting widespread commercialization of fuel cell technology are better performance and lower cost [2, 5].

The major costs of fuel cells are the electrolytes, catalysts, and storage. Phosphoric acid fuel cells (PAFCs) and proton exchange membrane fuel cells (PEMs) are the most widely used and most efficient. A fuel cell PEM engine costs $500/kW, compared to $50/kW for a gasoline engine leading to a total price of approximately $100,000 for an automobile running on fuel cells [1].

There are five families of fuel cells (FC). These are phosphoric acid fuel cells, proton exchange membrane (PEM) fuel cells, alkaline fuel cells, molten carbonate fuel cells, and solid oxide fuel cells; each have their own advantages and disadvantages. Significant progress has been made with hydrogen PEM fuel cells in the last decade. This thesis research will focus on polymer electrolyte membrane fuel cells (PEMFC).

A proton exchange membrane or polymer electrolyte membrane (PEM) is a semipermeable membrane generally made from ionomers and designed to conduct protons while being impermeable to gases such as oxygen or hydrogen. This is their essential function when incorporated into a membrane electrode assembly (MEA) of a proton exchange membrane fuel cell or of a proton exchange membrane electrolyser: separation of reactants and transport of protons. PEMs can be made from either pure polymer membranes or from composite membranes where other materials are embedded in a polymer matrix. One of the most common and commercially available PEM materials is the fluoropolymer (PFSA) Nafion, a DuPont product. While Nafion is an ionomer with a perfluorinated backbone like Teflon, there are many other structural motifs used to make ionomers for proton exchange membranes. Many use polyaromatic polymers while others use partially fluorinated polymers [6].

Nafion® is the most widely proton exchange membrane used for both PEMFC and DMFC systems. Nafion® is based on sulfonated fluorocarbon polymer and shows good thermal stability and high proton conductivity as advantages, while high methanol permeability (methanol crossover), high cost (about 900-1000 US $/m^2) and proton conductivity loss above 100 °C represent the disadvantages. Therefore, several studies have been carried out to identify different types of non-fluorinated polymers as alternative to the Nafion® and and in some case, comparable performances to the Nafion® in terms of proton conductivity and thermo-chemical properties, as well as lower crossover and costs [2].

Polyvinyl chloride, commonly abbreviated PVC, is the third-most widely produced plastic, after polyethylene and polypropylene and inconstruction because it is cheaper and stronger than more traditional alternatives such as copper or ductile iron[7]. PVC has high hardness and mechanical properties. The mechanical properties enhance with the molecular weight increasing, but decrease with the temperature increasing. The mechanical properties of rigid PVC (UPVC) is very good, the elastic modulus can reach to 1500-3,000 MPa. The soft PVC (Flexible PVC) elastic is 1.5-15 MPa. However, the elongation at break is up to 200% -450%. PVC friction is ordinary, the static friction factor is 0.4-0.5, the dynamic friction factor is 0.23[8]. 2-Acrylamido-2-methylpropane sulfonic acid (AMPS) is a reactive, hydrophilic, sulfonic acid acrylic monomer used to alter the chemical properties of wide variety of anionic polymers. In the 1970s, the earliest patents using this monomer were filed for acrylic fiber manufacturing. Today, there are over several thousands patents and publications involving use of AMPS in many areas including water treatment, oil field, construction chemicals,hydrogels for medical applications, personal care products, emulsion coatings, adhesives, and rheology modifiers. The geminal dimethyl group and the sulfomethyl group combine to sterically hinder the amide functionality and provide both hydrolytic and thermal stabilities to AMPS-containing polymers. The sulfonate group gives the monomer a high degree of hydrophilicity and anionic character at wide range of pH. In addition, AMPS is absorbing water readily and also imparts enhanced water absorption and transport characteristics to polymers [9]. Atom transfer radical polymerization (ATRP) is one of the controlled free radical polymerization techniques. ATRP is one of the most versatile methods for synthesizing homopolymers and copolymers with

predetermined molecular weights and narrow molecular weight distributions. It is based on the combination of an organic halide initiator (RX) with a metal/ligand catalytic system, which is able to promote fast initiation compared to propagation and then reversibly activate halogenated chain, ends (P*n*X) during polymerization.

During the last 20 years, living/controlled radical polymerization has allowed researchers to successfully pursue one of the main goals in macromolecular development, namely the synthesis of new polymers with well-defined chemical structures, control of the molecular weight, and low polydispersity. Photopolymerization has some advantages over thermally initiated polymerization. This is evidenced in the rapid growth of radiation curing as an industrial process, which depends on the use of photoinitiators. Photoinitiators can be used in controlled radical reactions. The use of N, N-diethyl dithiocarbamate (DDC) derivatives as so-called photoiniferters during radical polymerization reactions has been reported. The term iniferter is used as first coined by Otsu, meaning substances that act as initiator, transfer agent and terminator in radical polymerization reactions [47].

In this study, P(VC-*g*-AMPS) graft copolymer was were synthesized by using ATRP and iniferter methods. PVC backbone as macroinitiator and 2-Acrylamido-2-methylpropane sulfonic acid (AMPS) as sulfonic acid groups containing monomer were used. For iniferter method, sodium diethyl dithiocarbomate was used as photoinitiator.

The proton conductivity and thermal stability in copolymer have been investigated for PVC based membranes.

2. THEORETICAL PART

2.1 Fuel Cells

Fuel Cells are electrochemical devices that directly convert the chemical energy of a fuel into electricity.

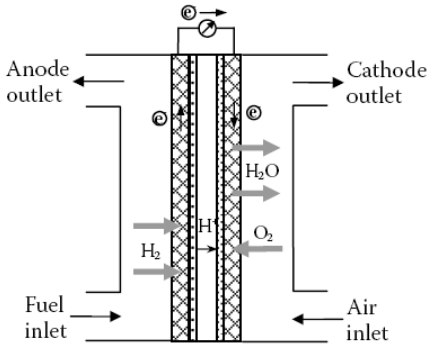

Figure 2.1 : Schematic of PEM fuel cell.

A fuel cell is an electrochemical energy conversion device. Current methods for the conversion of chemical energy to electrical energy are rather cumbersome and wasteful. Typically, coal is burned in a boiler to generate steam, the steam goes through a turbine, the turbine drives a generator, and the generator produces electricity. This whole process wastes about 60% of the energy originally in the coal. More energy is wasted in transmitting electricity through power lines to users. It is easy to see the desirability of converting chemical energy directly to electricity. This can be done in fuel cells [10]. It produces electricity from external supplies of fuel (on the anode side) and oxidant (on the cathode side). These react in the presence of an electrolyte. Generally, the reactants flow in and reaction products flow out while the electrolyte remains in the cell. Fuel cells can operate virtually continuously as long as the necessary flows are maintained as seen in Figure 2.1.

Fuel cells are very useful as power sources in remote locations, such as spacecraft, remote weather stations, large parks, rural locations, and in certain military applications. A fuel cell system running on hydrogen can be compact, lightweight and has no major moving parts [2].

2.1.1. Introduction and historical development

The concept of a fuel cell was proposed about 170 years ago when William Robert Grove conceived the first fuel cell in 1839, which produced water and electricity by supplying hydrogen and oxygen into a sulfuric acid bath in the presence of porous platinum electrodes. Unfortunately, there were no practical fuel cells developed for the following 120 years until Dr. Francis Bacon demonstrated a 5kW fuel cell for powering a welding machine in 1959, where an inexpensive nickel electrode and less corrosive alkaline electrolyte were used. One of the most important milestones in fuel cell history is an invention of polymer electrolyte membrane (PEM) in 1955 when Willard Thomas Grubb in General Electric (GE) modified the original fuel cell design with a sulfonated polystyrene ion-exchange membrane as the electrolyte. Better polymer electrolyte material, sulfonated tetrafluorethylene copolymer (Nafion®), was discovered in late 1960s by Walther Grot at DuPont. With its excellent thermal and mechanic stability, Nafion® became the most widely used electrolyte material for PEM fuel cells. The use of solid polymer electrolyte membrane has established the base for the modern fuel cell technology because the fuel cell with polymer electrolyte membrane is much simpler and more reliable than that of using liquid electrolyte. The second important factor in fuel cell history is the development of electrode catalysts for oxygen reduction and fuel oxidation. Much effort has been made to seek non-platinum catalysts, such as metalloporphyrins and metallo-phthalocyanines for catalytic oxygen reduction. Up tothe present, electrode catalysts and electrolyte membranes are still the major challenges in fuel cell research and development.

The electrolysis of water was tried at around the same time and the reverse reaction must have been tried. Sir W. Grove produced the first fuel cell experiment in 1839 as shown in Figure 2.2. He firstly electrolysed water to evolve hydrogen and oxygen in several electrolysers and then the power source was removed from the electrolysers. He showed that the electrolysers reversely generate electricity on the electrodes of each electrolyser. Then all the electrolysers were connected directly and the output power from the electrolysers was given to electrolyse water in another electrolyser. He showed that the electrolysis and generation of electricity takes place reversibly. About 130 years after Sir W. Grove's experiments, much attention was paid to the development of fuel cells, mostly for limited purposes, i.e., space shuttles or

submarines. Nowadays fuel cells are a necessary power source for the space shuttles [4,5].

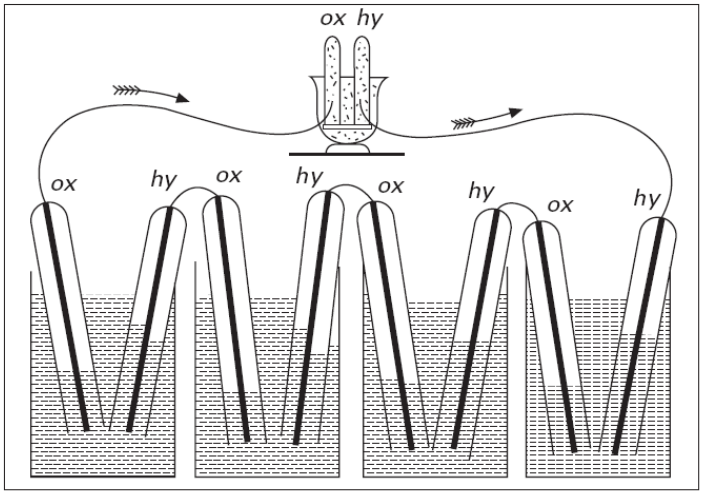

Figure 2.2 : Grove's fuel cell experiment.

2.1.2 Fuel cell systems

For practical application, a number of single fuel cells connected in series form a fuel cell stack to gain higher voltage and power including fuel cell stacks, pumps, batteries, sensors, fuel cartridge and electronic controller.

In the following pages, a brief overview of the basic electrochemical processes in a H_2/O_2 PEM fuel cell is given, followed by information on individual fuel cell components: anode, cathode, catalyst support, membrane, GDLs, and bipolar plates [6]. It has been seen that many chemical reactions can be regarded as the transfer of electrically charged electrons from one atom to another. Such a transfer can be arranged to occur through a wire connected to an electrode in contact with atoms that either gain or lose electrons. In that way, electricity can be used to bring about chemical reactions, or chemical reactions can be used to generate electricity [11].

For economic reasons, air is usually used as the cathode feed rather than pure O_2. Electrons are carried from the anode to the cathode through the external electric circuit. The anode and cathode electrode layers are typically made of Pt or Pt alloys dispersed on a carbon support for maximum catalyst utilization. Ionomers and polytetrafluoroethylene (PTFE) resins can be added to the electrode layers.

GDLs are made of porous media such as carbon paper or carbon cloth to facilitate the transport of gaseous reactants to the electrode layers, as well as the transport of

electrons and water away from the electrode layers. An MEA is sandwiched between two bipolar plates to form a single fuel cell. The word *bipolar* refers to a plate's bipolar nature in a series of single cells (known as a stack) in which a plate (or a set of half plates) is anodic on one side and cathodic on the other side.

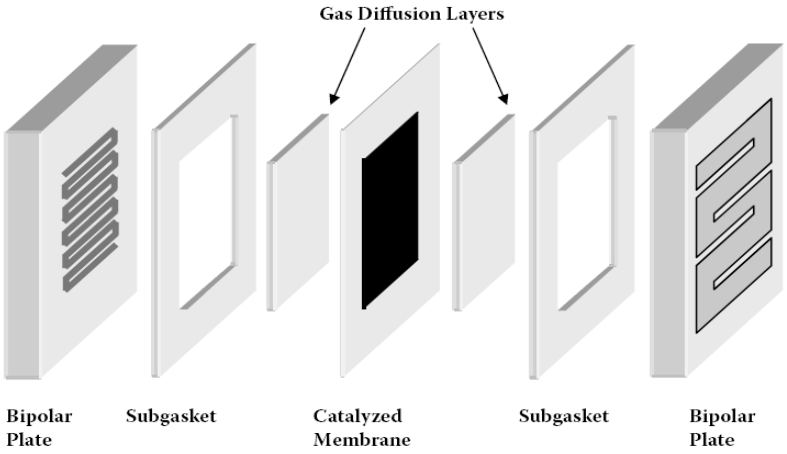

Figure 2.3 : Schematic views of a PEM fuel cell and a seven-layered MEA.

Figure 2.3 is a schematic view of a typical PEM fuel cell components [6]. A membrane electrode assembly (MEA) usually refers to a five-layer structure that includes an anode gas diffusion layer (GDL), an anode electrode layer, a membrane electrolyte, a cathode electrode layer, and a cathode GDL. Most recently, several MEA manufacturers started to include a set of membrane sub gaskets as a part of their MEA packages. This is often referred to as a seven-layer MEA. In addition to acting as a gas and electron barrier, a membrane electrolyte transports protons (H^+) from the anode, where H_2 is oxidized to produce H^+ ions and electrons, to the cathode, where H^+ ions and electrons recombine with O_2 to produce H_2O [6].

2.1.3 Types of fuel cell

Many types of fuel cell have been investigated. According to the characteristics of the electrolytes, they are divided into roughly five types: alkaline (AFC), phosphoric (PAFC), molten carbonate (MCFC), solid oxide (SOFC), and polymer electrolyte (PEFC). Much attention has been devoted to PEFC including direct methanol fuel cell (DMFC) recently. The features of such fuel cells are listed in Table 2.1.

Among all kinds of fuel cells, proton exchange membrane (PEM) fuel cells are compact and lightweight, work at low temperatures with a high output power density

and low environmental impact, and offer superior system startup and shutdown performance. These advantages have sparked development efforts in various quarters of industry to open up new field of applications for PEM fuel cells, including transportation power supplies, compact cogeneration stationary power supplies, portable power supplies, and emergency and disaster backup power supplies.

2.1.4 Application of fuel cell

Nowadays, such FCs are in different stages of development and have different applications. The only practical application of low temperature fuel cells considered in this chapter are AFCs in the American space shuttles. On the other hand, PAFCs have been used in stationary power generation plants since the 70s. Finally, PEFCs have experimented a resurgence in the 90s due to their performance improvement, as a consequence of the use of a new proton exchange membrane (Nafion®) and new techniques that enhanced the efficiency of platinum catalyst in the electrodes. This resurgence has been mainly directed towards portable and transport applications rather than stationary applications.

Industrial vehicles powered by 10 kW to 50 kW PEM fuel cells. These vehicles include forklifts and people movers. Hydrogen is the fuel of choice for these applications. Automotive PEM fuel cells with PEM systems power ratings from 50 kW to 100 kW. PEM systems with power ratings from 100 kW to 300 kW for heavy-duty vehicles such as buses. Hydrogen is the fuel of choice for these applications [12].

Recently a number of venture corporations put small fuel cells for stationary use out to the public. At home, we require electricity and heat. Typical Japanese housing consumes 4-5 kW of electricity in the daytime and around 1 kW at night. The PEFCs generate electricity and heat at the same time. Therefore, if 1 kW PEFC is installed in each home, it gets enough warm water all day round.

The major target of the PEFC is electric vehicles. If a large amount of the vehicles in the city area are replaced by fuel cell cars, clean atmospheric conditions would no doubt result. Fuel cells of 70–90 kW will be installed for standard type cars and about 200 kW is required for buses.

Most big motor companies such as Toyota, Honda, Nissan, GM, Ford, Daimler Chrysler, Hyundai and Volkswagen joined the California Fuel Cell Partnership car

rally that started in 1999 and ended its phase I in 2003. Phase II started in 2004 and will last until 2007. They have tested the fuel cell operation on board and the hydrogen stand and other subsidiary appliances.

The Japanese government bought several fuel cell cars in 2002 and is now using them for commuting purposes in the inner-city area. These are the first commercialized cars of this sort in the world [5].

2.2 Polymer Electrolyte Membrane Fuel Cell (PEMFC)

2.2.1 Introduction of PEMFC

This type of fuel cell consists of a gas diffusion layer and an electrode on each side and a polymer electrolyte membrane in between the electrodes. The electrode-membrane assembly is usually constructed in between the pressurized hot plates. [5]. Reactants enter the cell through gas channels, which are embedded in the current collectors (bipolar plate). The gas diffusion layers (GDL) are used to uniformly distribute the reactants across the surface of the catalyst layers (CL), as well as to provide an electrical connection between the catalyst layers and the current collectors.

The electrochemical reactions that drive a fuel cell occur in the catalyst layers which are attached to both sides of the membrane. The catalyst layers must be designed in such a manner as to facilitate the transport of protons, electrons, and gaseous reactants. Protons, produced by the oxidation of hydrogen on the anode, are transported through ion conducting polymer within the catalyst layers and the membrane. Electrons produced at the anode are transported through the electrically conductive portion of the catalyst layers to the gas diffusion layers, then to the collector plates and through the load, and finally to the cathode.

On the anode surface, hydrogen is oxidized to proton and the proton migrates to the cathode surface through the electrolyte membrane. On the cathode, oxygen is reduced in the presence of proton to water.

at the anode: $H_2 \rightarrow 2H^+ + 2e^-$

at the cathode: $2H^+ + 1/2O_2 + 2e^- \rightarrow H_2O(l)$

total reaction: $H_2 + 1/2O_2 \rightarrow H_2O(l)$

2.2.2. Commercial proton exchange membranes for fuel cell

2.2.2.1 General

Perfluorinated membranes are still regarded as the best in the class for PEM fuel cell applications. These materials are commercially available in various forms from companies such as DuPont, Asahi Glass, Asahi Chemical, 3M, Gore, and Solvay. Perfluorosulfonic acid (PFSA) polymers all consist of a perfluorocarbon backbone that has side chains terminated with sulfonated groups.

Today, the most widely used membrane electrolyte is DuPont's Nafion®. Due to its good chemical and mechanical stability in the challenging PEM fuel cell environment. A perfluorinated polymer with pendant sulfonated side chains, Nafion® was initially developed in 1968 by Walther G. Grot of DuPont for the chlor-alkali cell project of the National Aeronautics and Space Administration (NASA) space program.

The rate of PFSA degradation depends strongly on fuel cell operating conditions such as RH, temperature, H_2/O_2 crossover rate, CO concentration, air bleed level, and electrode potential.

Peroxide radicals from decomposition of H_2O_2 are believed to be responsible for membrane chemical degradation. The generally accepted end-group degradation mechanism, the so-called unzipping mechanism, starts from the end groups of a perfluorinated polymer chain.

2.2.2.2 Nafion®

One type of PEMs that meets most of these requirements is Nafion®. This is why Nafion® is the most commonly used and investigated PEM in fuel cells. The electrolyte consists of an acidic polymeric membrane that conducts protons but repels electrons, which have to travel through the outer circuit providing the electric work. A common electrolyte material is Nafion® from DuPont™, which consists of a fluoro-carbon backbone, similar to Teflon, with attached sulfonic acid SO_3 groups (see Figure 2.4). The membrane is characterized by the fixed-charge concentration (the acidic groups): the higher the concentration of fixed-charges, the higher is the protonic conductivity of the membrane. Alternatively, the term "equivalent weight" is used to express the mass of electrolyte per unit charge.

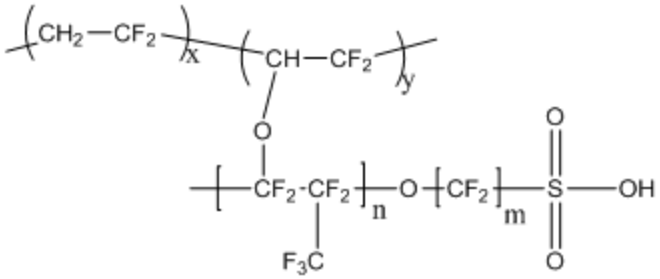

Figure 2.4 : Chemical structure of Nafion® (DuPont).

A perfluorosulfonic polymer such as Nafion® naturally combines, in one macromolecule, the extremely high hydrophobicity of the perfluorinated backbone with the extremely high hydrophilicity of the sulfonic acid functional groups. Especially in the presence of water, this gives rise to a hydrophobic/hydrophilic regions' separation. The sulfonic acid functional groups aggregate to form a well connected hydrophilic domain, which is responsible for the protons and water transport. Vice versa, the hydrophobic domain provides the polymer with the morphological stability and prevents the polymer dissolving in water.

2.2.3 Proton conductivity

The role of the membrane in the fuel cell is to conduct protons whilst separating the gases and acting as an electronic insulator. In PEM fuel cells, proton conductivity is almost always provided by sulfonic acid groups chemically bound to a polymer chain. This type of membrane requires water to conduct protons. The most commonly used commercial materials are perfluorinated polymers such as Nafion. Nafion requires a minimum of 2-3 molecules of water per sulfonic acid group for dissociation; increasing the water content beyond this increases the hydration and proton mobility is enhanced. In the fully swollen state, after immersion in boiling water, the membrane is plasticized and proton conduction is at its most rapid. At high temperatures and low relative humidity, the water content of the membrane drops and conduction becomes more challenging. One way of reducing the reliance on water would be to increase the acidity of the sulfonic acid group and thus facilitate dissociation. Perfluorinated sulfonated polymers, however, are already highly acidic (i.e. superacidic)4 and increasing the acidity further would be difficult. Sulfonimides alone have been claimed to possess higher acidity than the CF3SO3H groups present in Nafion type materials.

Another way to increase proton conduction at low water contents is to reduce the distance between sulfonic acid groups, enabling easier transport. This could be accomplished by increasing the concentration of sulfonic acid groups in the membrane. This approach is limited by the requirement of the membrane to remain insoluble. However, the most advanced commercial membranes do have higher sulfonate concentrations (lower equivalent weights) than the well established Nafion 1100 ionomer.

2.2.4 Water management

In the high temperature low RH environment, effective use of available water is essential. Water is provided by the partially hydrated fuel and oxidant gas feeds, and by the oxygen reduction reaction. Water is lost from the cell through the exhaust gases. Inside the Membrane Electrode Assembly, water is distributed by electro osmotic drag whereby each proton drags water with it from anode to cathode and by diffusion from cathode to anode due to the water concentration gradient. This is shown schematically in Figure 2.5. The electro-osmotic drag of most sulfonic acid membranes has been shown to be close to one in the presence of water vapour with little variation between membrane types. To ensure the most even water distribution, a membrane enabling rapid water back diffusion from cathode to anode is therefore essential.

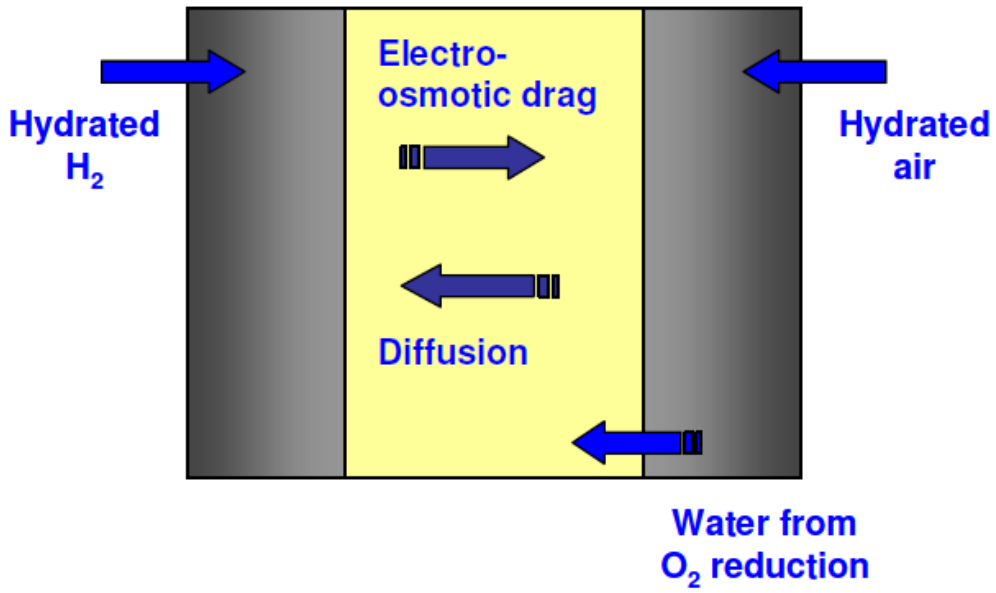

Figure 2.5: Water management.

2.3 Living Polymerization

The considerable attention to the field of living polymerization techniques is due to the increasing demand for well-defined functional polymers with fully controllable molecular characteristics. Living polymerization, the concept of which was first introduced by Szwarc in 1956, is one of the most promising ways for the synthesis of well-defined polymers [34, 35]. A living polymerization is defined as a chain polymerization that proceeds in the absence of chain transfer and chain termination as indicated by Szwarc. His pioneering work on the anionic polymerization of St initiated with sodium naphthalenide opened the field of living polymers with controlling the molecular weight and molecular weight distributions as well as the structure of the end-groups.

After the discovery of living anionic polymerization, critical research on cationic polymerization was performed in the "living" era**.** An equimolar mixture of HI/I_2 was the first system used for the initiation of such polymerizations of vinyl ethers [36]**.** In this system, the initially formed adduct of HI to a vinyl ether is activated by iodine. The fast initiation realized ideal living cationic polymerization of alkyl vinyl ethers. Thus, homopolymers and block copolymers with narrow molecular weight distributions were first synthesized in cationic polymerization.

Since then, much progress has been made in these living ionic polymerization techniques and polymerization of various monomers have been examined, for which numerous types of initiators have been developed. While these techniques are undoubtedly successful, they do suffer from rigorous synthetic requirements including the use of very pure reagents and the total exclusion of water and oxygen and incompatibility with a variety of functional monomers. Definitely, with so many parameters to control, such requirements represent a grand challenge to synthetic polymer chemists and somewhat delay their practical use. Aware of the intrinsic limitations of ionic polymerizations, many efforts have been made to find new routes which could address the development of a free radical polymerization. This process is tolerant to impurities, very versatile with respect to compatibility with broad range of functional monomers, and relatively easy to implement in an industrial plant.

2.4. Controlled / Living Radical Polymerization

Today, conventional free-radical polymerization (FRP) is still one of the most widely applied processes for the preparation of polymeric materials as nearly 50% of all commercial synthetic polymers are produced by this method. The main reason for this fact is that a wide range of monomers can be polymerized and copolymerized via radical chemistry, which provides a spectrum of materials for various markets. Moreover, the polymerization does not require rigorous process conditions. On the other hand, some important elements of the polymerization process that would lead to the well-defined polymers with controlled molecular weight, polydispersity,composition, structural architecture, and functionality are poorly controlled. The importance of the synthesis of polymers with such control has been augmented due to the rising demands for the specialty polymers. Obviously, living polymerization is an essential technique for synthesizing polymers with controlled structures. Moreover, living polymerization techniques allow preparation of macromonomers, macroinitiators, functional polymers, block and graft copolymers, and star polymers. In this way, the need for specialty polymers having a desired combination of properties can be fulfilled. Control of complex architectures by living polymerization has largely been achieved using living anionic and cationic as well as group transfer polymerization techniques. From the practical point of view, however, these techniques are less attractive than free-radical polymerization, because the latter can be performed much more easily. Moreover, ionic techniques are limited to a very few vinyl monomers, whereas practically all vinyl monomers can be homo and copolymerized by a free-radical mechanism long-lasting goal has been the development of controlled/living radical polymerization methods. As mentioned previously, radical polymerization suffers from some defects (i.e., the control of the reactivity of the polymerizing monomers and, in turn, the control of the structure of the resultant polymer). In ionic living systems, however, the chain ends do not react with one another due to the electrostatic repulsion. On the other hand, the growing radicals very easily react with each other at diffusion controlled rates via combination and/or disproportionation. Therefore, controlled/living radical polymerization has long been considered impossible. Following the discovery of living anionic and cationic polymerization, many attempts have been made to find controlled/living radical polymerization systems to achieve a high level of control

over molar mass, polydispersity, end groups, and architecture. Despite considerable progress, a truly controlled/living radical polymerization has not been developed until a little more than a decade ago. In the past decade, a number of controlled/living radical polymerization methods have been developed and the three most promising types are: atom transfer radical polymerization (ATRP) (also known as transition metal catalyzed radical polymerization), stable freeradical polymerization (SFRP) (also known as nitroxide-mediated polymerization, NMP), and reversible addition-fragmentation chain transfer (RAFT) polymerization. This chapter focuses on the recent progress on these three methods and the earlier attempts will not be considered here as they were discussed in detail in the first edition of the book [14].

2.4.1 Atom transfer radical polymerization (ATRP)

2.4.1.1 About ATRP

Atom Transfer Radical Polymerization (ATRP) is among the most effective and most widely used methods of controlled radical polymerization (CRP). ATRP allows scientists to easily form polymers by putting together component parts, called monomers, in a controlled, piece-by-piece fashion. Assembling polymers in such a manner has allowed scientists to create a wide range of polymers with highly specific, tailored functionalities. For example, polymers created using ATRP have been used for coatings and adhesives, and are currently under investigation for use in the medical and environmental fields.

Until the discovery of ATRP, polymer chemists were severely limited in their ability to control the composition and architecture of macromolecules, making it difficult to provide materials with highly specific, uniform characteristics. Since the mid-1950s, many chemists attempted to develop a “living” or controlled polymerization process that would create well-defined polymers in a simple, inexpensive manner. In the mid-1990s, several laboratories across the world surmounted this vexing problem by developing CRP methods. These techniques allow synthesis of fundamentally new materials with complex, well-defined nanoscale architectures. In 1995, Carnegie Mellon University Professor Krzysztof Matyjaszewski discovered one of the first — and most robust — CRP methods, ATRP. The seminal paper was published in the Journal of the American Chemical Society and has been cited close to 3,000 times and the initial 1995 patent applications close to 200 times.

ATRP differs significantly from earlier conventional radical based polymer manufacturing methods by allowing scientists to produce complex polymer structures using a special catalyst that adds one or a few subunits (monomers) at a time to a growing polymer chain. This living, synthetic process can be shut down or re-started at will, depending on how the temperature and other conditions of the reaction are varied. ATRP is an exceptionally robust way to uniformly and precisely control the chemical composition and architecture of polymers as well as the uniform growth of every polymer chain, while employing a broad range of monomers.

Key to ATRP's success is that the process is easily conducted in available industrial equipment. Much of its research progress and commercial success can be attributed to two research consortia Matyjaszewski has initiated and led. These two highly successful consortia have allowed companies to quickly incorporate the latest ATRP methodologies into the development of new products for their specific markets. These consortia have comprised more than 40 multinational chemical companies from across the world who have sent their employees to be trained in Matyjaszewski's laboratory.

ATRP technology developed by Matyjaszewski has already been licensed to nine international companies, which started production of ATRP-based polymers in Japan, Europe and the United States in 2004. ATRP has been successfully used to create better pigment dispersants for inkjet printing, cosmetics, chromatographic packings, adhesives and sealants for self-cleaning windows, among others. Some other applications that are being evaluated include drug delivery methods, coatings for cardiovascular stents, scaffoldings for bone regeneration, biocidal surfaces, degradable plastics and others in the optoelectronic and automotive industries [15].

2.4.1.2 Kinetics and mechanism of ATRP

ATRP was developed by designing a proper catalyst (transition metal compound and ligands), using an initiator with an appropriate structure, and adjusting the polymerization conditions, such that the molecular weights increased linearly with conversion and the polydispersities were typical of a living process. This allowed for an unprecedented control over the chain topology (stars, combs, branched), the composition (block, gradient, alternating, statistical), and the end functionality for a large range of radically polymerizable monomers [18].

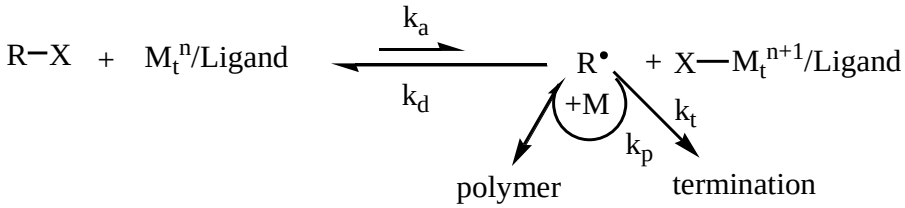

Figure 2.6: Mechanism for ATRP.

A general mechanism for ATRP is represented by (see Figure 2.6). The radicals, i.e., the propagating species Pn*, are generated through a reversible redox process catalyzed by a transition metal complex (activator, M_t^n –Y / ligand, where Y may be another ligand or a counterion) which undergoes a one-electron oxidation with concomitant abstraction of a (pseudo) halogen atom, X, from a dormant species, Pn–X. Radicals react reversibly with the oxidized metal complexes, X–M_t^{n+1} / ligand, the deactivator, to reform the dormant species and the activator. This process occurs with a rate constant of activation, k_a, and deactivation k_{da}, respectively. Polymer chains grow by the addition of the free radicals to monomers in a manner similar to a conventional radical polymerization, with the rate constant of propagation, k_p. Termination reactions (k_t) also occur in ATRP, mainly through radical coupling and disproportionation; however, in a well-controlled ATRP, no more than a few percent of the polymer chains undergo termination.

The rate of polymerization is first order with respect to monomer, alkyl halide (initiator), and transition metal complexed by ligand. The reaction is usually negative first order with respect to the deactivator (X-M_t^{n+1}/Ligand). The rate equation of copper-based ATRP is formulated in discussed conditions and given in (2.2). The apparent propagation rate constant, where k_p and K_{eq} refer to the absolute rate constant of propagation and the atom transfer equilibrium constant for the propagating species, respectively.

$$Rp = k_p^{app} (M) = k_p (R\bullet) (M) = k_p K_{eq} (I) ((CuX)/(CuX_2)) (M) \quad \textbf{(2.1)}$$

Figure 2.6 shows a typical linear variation of conversion with time in semi logarithmic coordinates (kinetic plot). Such a behavior indicates that there is a constant concentration of active species in the polymerization and first-order kinetics with respect to monomer.

However, since termination occurs continuously, the concentration of the Cu(II) species increases and deviation from linearity may be observed [16]. For the ideal

case with chain length independent from termination, persistent radical effect [17] kinetics implies the semi logarithmic plot of monomer conversion vs. time to the 2/3 exponent should be linear. Nevertheless, a linear semi logarithmic plot is often observed.

This may be due to an excess of the Cu(II) species present initially, a chain length dependent termination rate coefficient, and heterogeneity of the reaction system due to limited solubility of the copper complexes. It is also possible that self-initiation may continuously produce radicals and compensate for termination. Similarly, external orders with respect to initiator and the Cu(I) species may also be affected by he persistent radical effect [19].

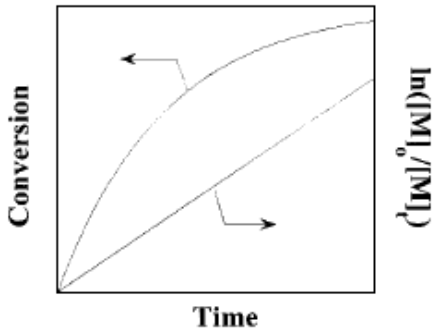

Figure 2.7 : Kinetic plot and conversion vs. time plot for ATRP.

Results from kinetic studies of ATRP for styrene (S) [20], methyl acrylate (MA) [21] and methyl methacrylate (MMA) [22-23] under homogeneous conditions indicate that the rate of polymerization is first order with respect to monomer, initiator, and Cu(I) complex concentrations. These observations are all consistent with the derived rate law.

It should be noted that the optimum ratio can vary with regard to changes in the monomer, counter ion, ligand, temperature, and other factors [22, 24]. The precise kinetic law for the deactivator CuX_2 was more complex due to the spontaneous generation of Cu(II) via the persistent radical effect [19-20].

In the atom transfer step, a reactive organic radical is generated along with a stable Cu(II) species that can be regarded as a persistent metallo-radical. If the initial concentration of deactivator Cu(II) in the polymerization is not sufficiently large to ensure a fast rate of deactivation (k_d(Cu(II))), then coupling of the organic radicals will occur, leading to an increase in the Cu(II) concentration.

Radical termination occurs rapidly until a sufficient amount of deactivator Cu(II) is formed and the radical concentration is low. Under such conditions, the rate at which radicals combine (k_t) will become much slower than the rate at which radicals react with the Cu(II) complex in a deactivation process and a controlled polymerization will proceed.Typically, a small fraction (~5 %) of the total growing polymer chains will be terminated during the early stage of the polymerization, but the majority of the chains (>95 %) will continue to grow successfully.

If the deactivation does not occur, or if it is too slow ($k_p >> k_d$), there will be no control and polymerization will become classical redox reaction therefore the termination and transfer reactions may be observed. To control the polymerization better, addition of one or a few monomers to the growing chain in each activation step is desirable. Molecular weight distribution for ATRP is given in (2.2).

$$M_w/M_n = 1 + ((k_d(RX)_0)/(k_p(X\text{-}M_t^{n+1}))) \times ((2/p)-1) \quad \textbf{(2.2)}$$

p = polymerization yield

$(RX)_o$ = concentration of the functional polymer chain

$(X\text{-}M_t^{n+1})$ = concentration of the deactivators

k_d = rate constant of deactivation

k_p = rate constant of activation

2.4.2 Components of ATRP

As a multicomponent system, ATRP includes the monomer, an initiator with a transferable (pseudo) halogen, and a catalyst (composed of a transition metal species with any suitable ligand). Both activating and deactivating components of the catalytic system must be simultaneously present. Sometimes an additive is used. For a successful ATRP, other factors, such as solvent and temperature, must also be taken into consideration.

2.4.2.1 Monomers

Monomers: In ATRP, a variety of monomers, such as styrenes, (meth)-acrylates, acrylonitrile, acrylamides, methacrylamides, N-vinylpyridine and diens can be used to obtained well-defined polymers. However, even under the same conditions using the same catalyst, each monomer has its own unique atom transfer equilibrium constant for its active and dormant species [25].

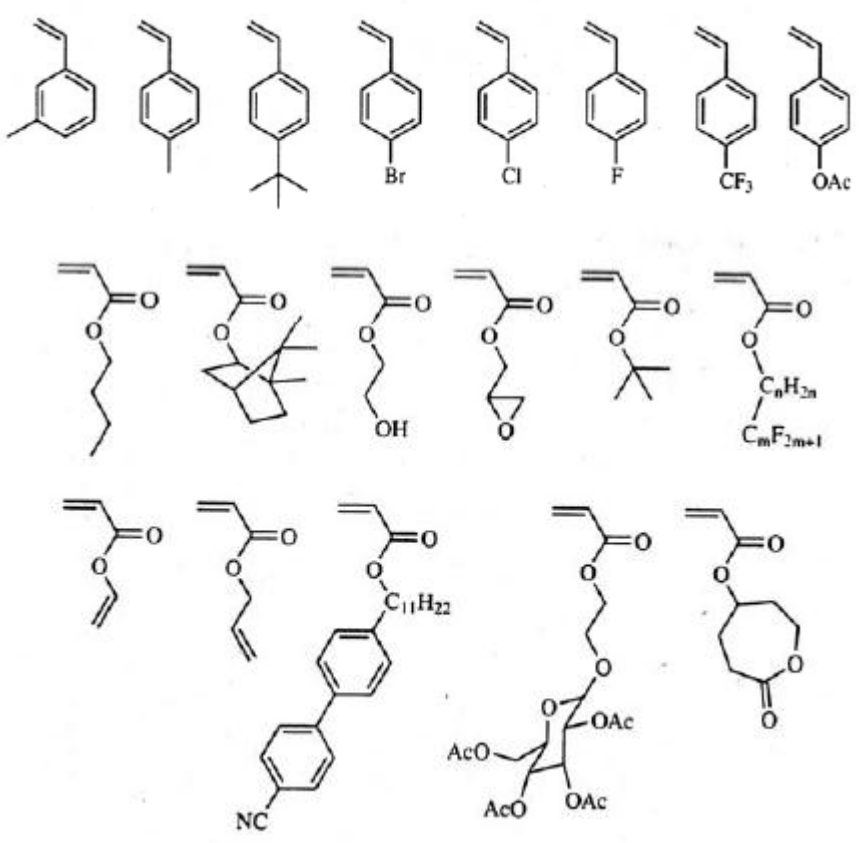

Figure 2.8 : Some of the monomers used in ATRP.

2.4.2.2 Initiators

The main role of the initiator is to determine the number of growing polymer chains. Two parameters are important for a successful ATRP initiating system. First, initiation should be fast in comparison with propagation. Second, the probability of the side reactions should be minimized.

Initiators: A variety of halogenated initiators and macro initiators activated by various types of aryl, sulfonyl and carbonyl groups can be used in ATRP systems. In ATRP, alkyl halides (R-X) are typically used as initiator (Table 2.3). If initiation is fast and transfer and termination negligible, then the number of growing chains is

constant and equal to the initial initiator concentration. The theoretical molecular weight or degree of polymerization (DP) increases reciprocally with the initial concentration of initiator at full monomer conversion.

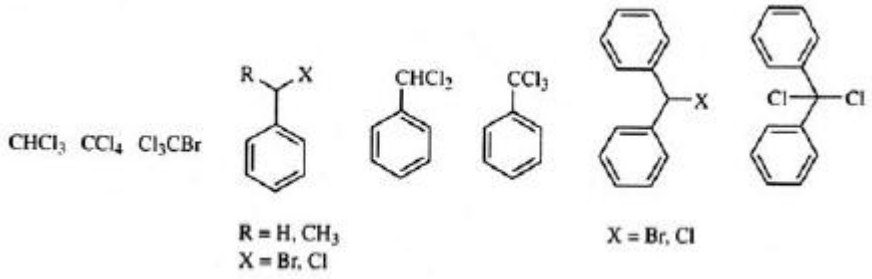

Figure 2.9 : ATRP initiators; halogenated alkanes and benzylic halides.

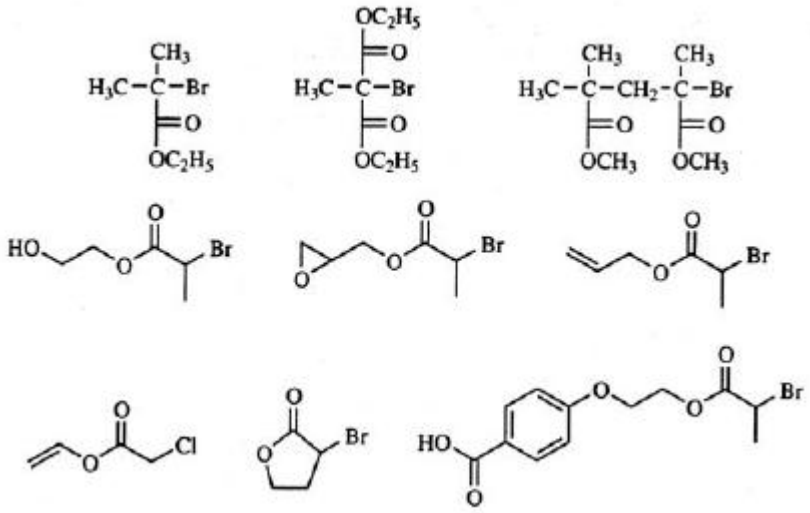

Figure 2.10 : ATRP initiators; α-bromoesters.

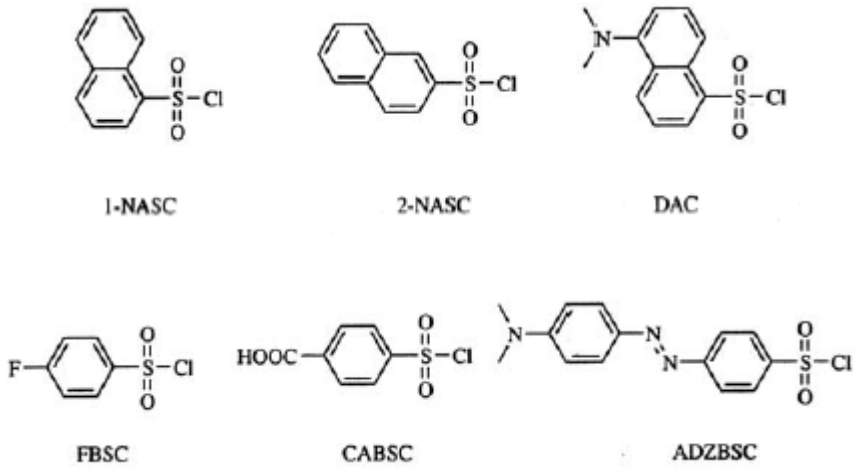

Figure 2.11 : ATRP initiators; sulfonyl chlorides.

2.4.2.3 Catalyst and transition metals

Perhaps the most important component of ATRP is the catalyst. It is the key to ATRP since it determines the position of the atom transfer equilibrium and the dynamics of exchange between the dormant and active species. There are several prerequisites for an efficient transition metal catalyst. The metal center must have at least two readily accessible oxidation states separated by one electron. The metal center should have reasonable affinity toward a halogen. The coordination sphere around the metal should be expandable on oxidation to selectively accommodate a (pseudo) halogen. The ligand should complex the metal relatively strongly. Eventually, the position and dynamics of the ATRP equilibrium should be appropriate for the particular system. To differentiate ATRP from the conventional redox-initiated polymerization and induce a controlled process, the oxidized transition metal should rapidly deactivate the propagating polymer chains to form the dormant species. A variety of transition metal complexes with various ligands have been studied as ATRP catalysts. The majority of work on ATRP has been conducted using copper as the transition metal. Apart from copper-based complexes, Fe, Ni, Ru, etc. have been used to some extent [16, 26].

2.4.2.4. Ligands

The main roles of the ligand in ATRP is to solubilize the transition metal salt in the organic media and to adjust the redox potential and halogenophilicity of the metal center forming a complex with an appropriate reactivity and dynamics for the atom transfer. The ligand should complex strongly with the transition metal. It should also allow expansion of the coordination sphere and should allow selective atom transfer without promoting other reactions. The most common ligands for ATRP systems are substituted bipyridines, alkyl pyridylmethanimines and multidentate aliphatic tertiary amines such as 1,1,4,7,7-pentamethyldiethylenetriamine (PMDETA), and tris(2(dimethylamino) ethyl)amine (Me_6-TREN).

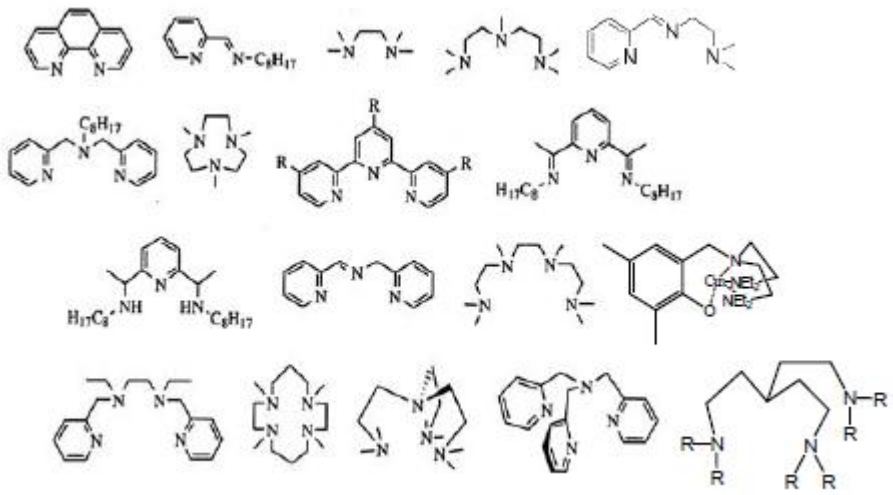

Figure 2.12 : Some of the ligands using ATRP.

2.4.2.5 Solvents

Solvents: ATRP can be carried out either in bulk, in solution, or in a heterogeneous system (e.g., emulsion, suspension). Various solvents, such as benzene, toluene, anisole, diphenyl ether, ethyl acetate, acetone, dimethyl formamide (DMF), ethylene carbonate, alcohol, water, carbon dioxide, and many others, have been used in the polymerization of different monomers.

2.4.2.6 Temperature and reaction times

The rate of polymerization in ATRP increases with increasing temperature due to the increase of both the radical propagation rate constant and the atom transfer equilibrium constant. As a result of the higher activation energy for the radical propagation than for the radical termination, higher k_p/k_t ratios and better control ("livingness") may be observed at higher temperatures. However, chain transfer and other side reactions become more pronounced at elevated temperatures. The optimal temperature depends mostly on the monomer, the catalyst, and the targeted molecular weight. Therefore, for successful ATRP, optimum temperature should be found depending on the monomer, catalyst and the other components of ATRP [16].

2.4.3 Iniferters

Iniferter is a useful and convenient method for the synthesis of vinyl polymers under mild reaction conditions, although the polymerization is *quasiliving* radical

polymerization. Photochemically or thermally activated polymerization can proceed in the presence of radically polymerizable vinyl monomers under appropriate reaction conditions through radical pair generation, monomer addition, and rapid recombination. The peculiar behavior of thiuram disulfides in free radical polymerization was first identified by Ferington and Tobolsky and. These molecules can act simultaneously as an *ini*tiator, chain trans*fer* agent, and*ter*minator in a polymerization reaction and generally referred as iniferters by anomy to their role and.

So far, many iniferters have been reported and utilized for the synthesis of telechelic polymers. Telechelic preparation is based on the concept of locating the required function on the alkyl group of the thiuram disulfide and using it in the photo or thermal polymerization. Since end groups are introduced via initiation and transfer and common bimolecular termination between two growing chains are negligible, perfect bifunctional telechelics are available along this route. Several functional disulfides and substituted tetraphenylethylenes were also used as iniferters in free radical polymerization. The functionalities of the telechelics prepared by iniferter method were reported to be close to 2, within experimental error. The formation of the nonfunctional polymers was claimed to be negligible because of the triple function of the iniferter. For example, carboxylic acid and amino functionalities were introduced to polystyrene using the corresponding disulfides. Diamino functional poly (*t*-butyl acrylate) was also prepared. In this case, polymers were readily hydrolyzed to polyacrylic acid possessing amino terminal groups, which is a useful material for the application of polyelectrolytes. The photochemically and thermally induced iniferter properties of the tetraalkylthiuram disulfides during free radical polymerization were also exploited to end functionalize poly(methyl methacrylate) and polystyrene [37].

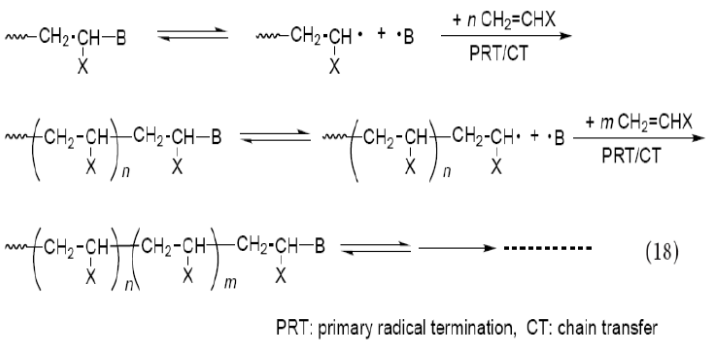

Figure 2.13: Mechanism of iniferters.

Primary radical termination, i.e., ordinary bimolecular termination is neglected, it is expected that a polymer will be obtained with two initiator fragments at the chain ends.

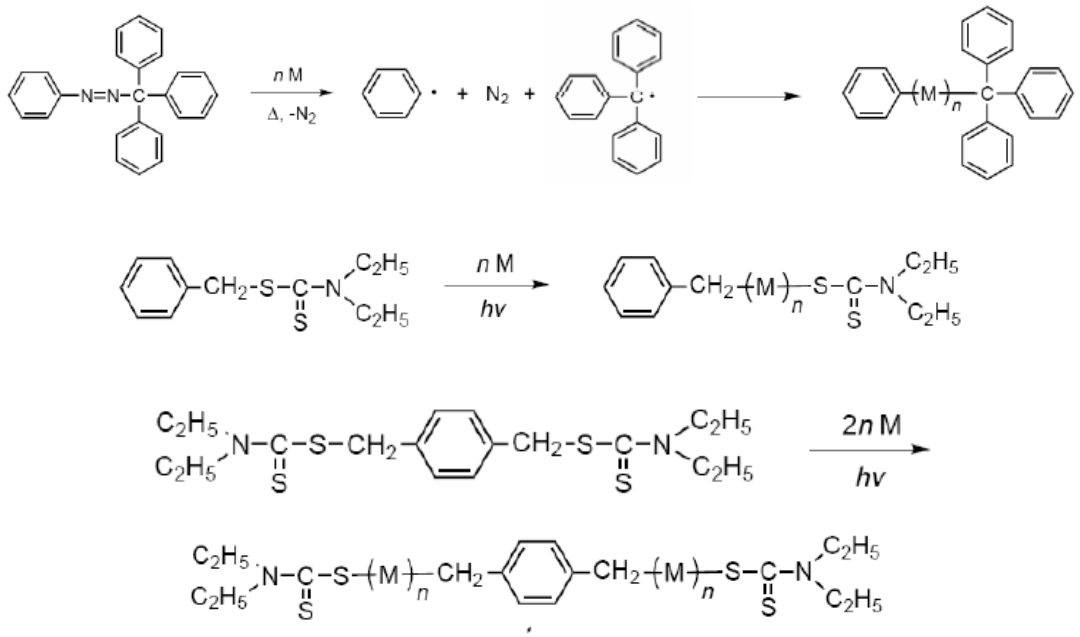

Figure 2.14: A-A or A-B type of iniferter.

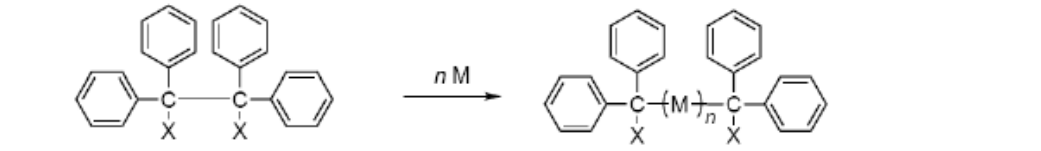

X = H, C_2H_5, -C_2H_4-, OC_6H_5, $OSi(CH_3)_3$, OH,$OCOCH_3$, OCH3, CH_3, $CO_2C_2H_5$, CN

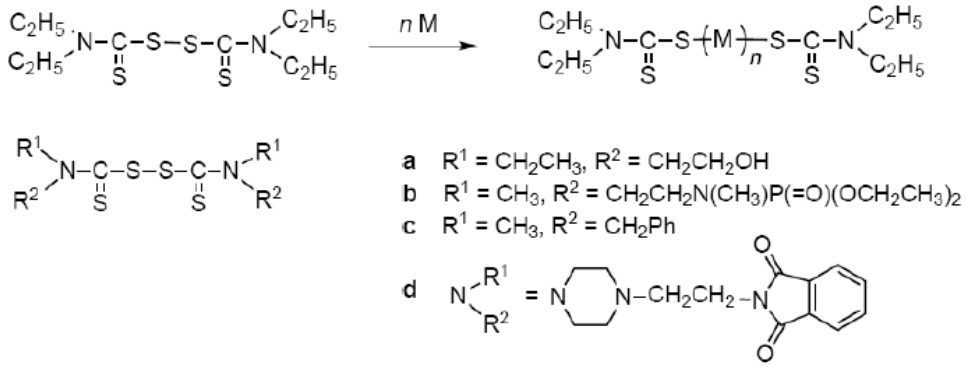

Figure 2.15: B-B type of iniferter.

2.4.4 Reversible addition–fragmentation chain transfer process (RAFT)

A subclass of C/LRP systems, reversible addition-fragmentation chain transfer (RAFT) polymerization, is one of the most extensively studied C/LRP methods [38]. RAFT polymerization is arguably the most adaptable of all the C/LRP techniques due to the ability of polymerizations to be conducted under a variety of conditions [39]. It is the most flexible technique with respect to monomer choice and functional group tolerance and allows for the construction of well-defined polymeric materials with complex architectures. Moreover, a distinct advantage of RAFT polymerization is its relative simplicity and versatility, since conventional free radical polymerizations can be readily converted into a RAFT process by adding an appropriate RAFT agent while other reaction parameters can be kept constant.

The selection of an appropriate RAFT agent for any particular monomer is probably the most crucial step in performing a successful RAFT polymerization. RAFT agent have in common to contain a thiocarbonylthio function, and their structure can be schemed as [Z-(C=S)S-R] (Figure 2.15), where the R and Z groups both play vital roles in a controlled/living fashion. The R group must be a better leaving group and efficiently reinitiate polymerization and the Z group should first activate the C=S bond toward radical addition and then stabilize the intermediate radical formed. RAFT agents can be categorized into four classes depending on the different substituent group next to the C=S functionality: dithioesters (Z = alkyl or aryl), trithiocarbonates (Z = SR), xanthates (dithiocarbonates) (Z = O-alkyl) and dithiocarbamates (Z = NR_2) (R = alkyl or H) (Figure 2.16) [40,41].

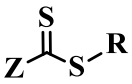

R	Z	Class of RAFT agent
$-CH_2CN$, $-CH_2Ph$	-Ph	Dithioseter
$-C(CH_3)_2(COOEt)$	$-C_nH_{2n+1}$	
$-C(CH_3)_2CN$	$-NEt_2$	Dithiocarbamate
$-C(CH_3)_2Ph$	-OEt	Xanthate (MADIX agent)
$-C(CH_3)_2CN$	$-SCH_3$	Trithiocarbonate

Figure 2.16: Main classes of RAFT agents.

Unlike ATRP and NMP, where the equilibrium between the dormant and active, propagating chains is based on reversible termination, RAFT polymerization is based on reversible or degenerate chain transfer.

The generally accepted mechanism for a RAFT polymerization is depicted in Figure 2.17 [42]. The first step of polymerization is the initiation step, where a radical is created and reacts with the monomer (step I). This growing polymer chain rapidly adds to the reactive [S=C(Z)SR] bond of the RAFT agent to form a radical intermediate (the radical initiator may add directly onto the RAFT agent, before reacting with any monomer). Step II shows the fragmentation of the intermediate occurring reversibly either toward the initial growing chain or to free the re-initiating group ($R^{\bullet}$) and a polymeric RAFT agent. The radical $R^{\bullet}$ can then re-initiate polymerization by reacting with the monomers or react back on the polymeric RAFT agent (step III). Once the initial RAFT agent has been entirely consumed, the polymeric RAFT agent is solely present in the reaction medium and enters equilibrium (IV). This equilibrium is considered the main equilibrium, and a rapid exchange between active and dormant (thiocarbonyl- thio capped) chains ensures equal probability for all chains to grow, therefore leading to the production of narrow polydispersity polymers. Although limited, termination reactions still occur v*ia* combination or disproportionation mechanisms (step IV). When the polymerization is complete, the great majority of the chains contain the thiocarbonylthio moiety as the end group which has been identified by ^{1}H NMR and UV–vis spectroscopy [43]. Additional evidence for the proposed mechanism was provided by the identification of the intermediate thioketal radical by electron spin resonance (ESR) spectroscopy [44].

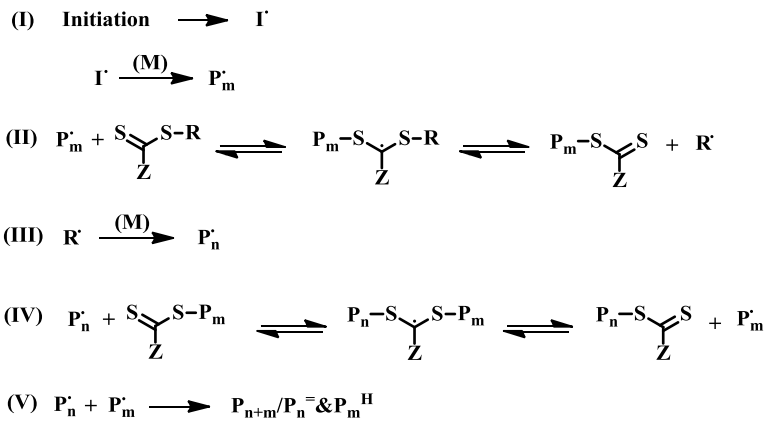

Figure 2.17: Proposed general mechanism of RAFT polymerization.

Many different sources of initiation have been reported for a RAFT polymerization, such as the thermal initiation, direct photochemical stimulation of the RAFT agent by ultraviolet light or γ radiation and by decomposition of organic initiators. The thermal decomposition of radical initiators is, however, the most widely adopted method of initiation, due to the commercial availability of such compounds. Polymerization temperature is usually in the range of 60–80 ^{o}C, which corresponds to the optimum decomposition temperature interval of the well-known initiator azobis(isobutyronitrile) (AIBN). However, even room temperature and high temperature conditions can also be applied. Generally, a RAFT agent/free-radical ratio of 1:1 to 10:1 yields polymers with narrow molecular weight distributions.

Photo- and γ-ray-induced reactions, which use light energy to generate radicals in RAFT polymerization, offer a number of advantages compared with thermally initiated ones. The major advantage is to allow the polymerization to be conducted at room temperature with relatively shorter reaction times. In photoinduced reactions, however, the RAFT agent should carefully be selected, as in some cases control over the molecular weight cannot be attained, particularly at high conversions because it may also decompose under UV light. γ-Ray-induced RAFT polymerization appeared to be more penetrating compared with the corresponding UV-induced processes.

2.5 Graft Copolymer

Graft polymers refer to the special type of branched polymers in which branched chains are structurally distinct from the main chain. The main chain is commonly called as the backbone and the branches as the side chains which are distributed along the backbones either randomly or uniformly.

When graft polymers characterized by a high density of grafted chains they were named ‘‘macromolecular brushes’’. In terms of chemical composition, macromolecular brushes can be categorized into homopolymer brushes and copolymer brushes. The latter typically consist of two or more types of polymer side chains. When only two types of polymer grafts are involved, they can be arranged in a random, alternating, block, and “centipede” manner [15].

Graft copolymers have been the subject of continuously increasing interest due to their unique specific properties (morphology, phase behaviour, etc.). In general, graft copolymers can be prepared following three main strategies: (a) the “*grafting*

through", (b) the "*grafting from*", and (c) *the* "*grafting tonto*" strategies which differentiate from each other based on the formation principle. The different pathways are schematically depicted in Figure 2.18.

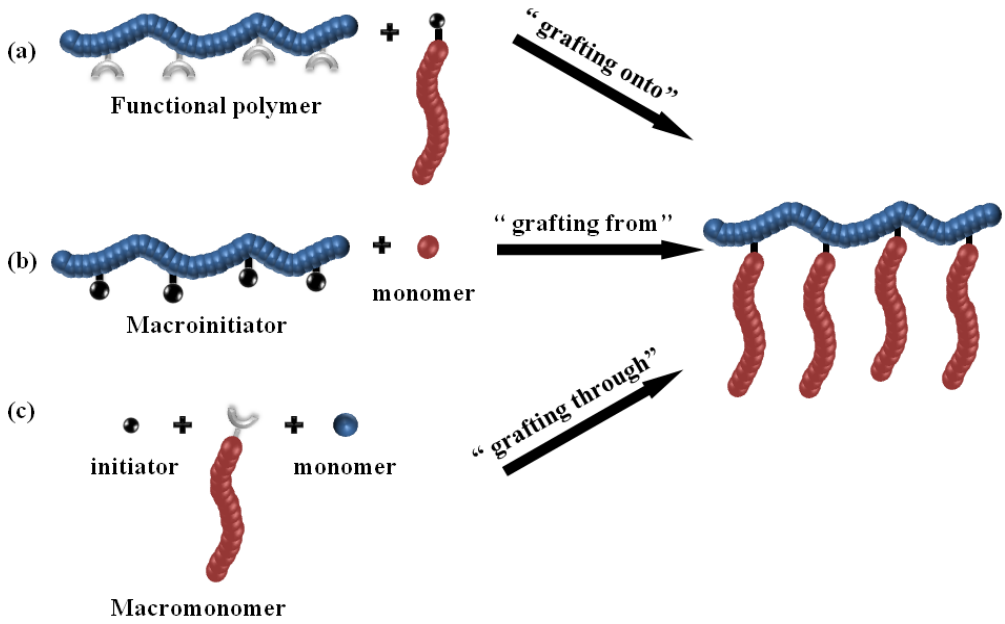

Figure 2.18: Strategies for the synthesis of graft copolymer: (a) ''grafting onto'', (b) ''grafting from'', and (c) ''grafting through''.

The ''*grafting onto*'' strategy involves the attachment of preformed polymer chains via chemical reaction with reactive side chains of a polymer backbone. Secondly, the ''*grafting from*'' strategy, consists in a polymerization of the grafts from a polymer backbone bearing initiating sites. The last approach is the ''grafting through'' strategy which relies on polymerization of appropriate macromonomers.

2.5.1 Grafting through

The "grafting through" method (or macromonomer method) is one of the simplest ways to synthesize graft copolymers with well defined side chains.

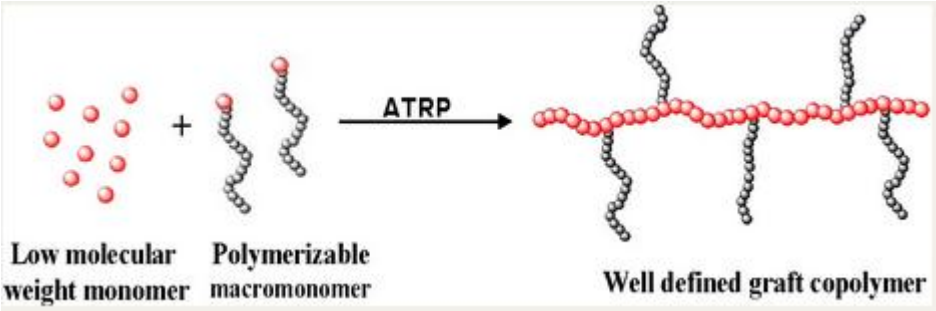

Figure 2.19: Grafting through via ATRP.

Typically a low molecular weight monomer is radically copolymerized with a (meth)acrylate functionalized macromonomer. This method permits incorporation of macromonomers that have prepared by other controlled polymerization processes into a backbone prepared by a CRP.

Moreover, it is possible to design well-defined graft copolymers by combining the CRP "grafting through" macromonomers procedure where the macromonomers had been prepared by any controlled polymerization process. This combination of controlled polymerization processes allows control of polydispersity, functionality, copolymer composition, backbone length, branch length and branch spacing by consideration of mole-ratio of the MM in the feed and reactivity ratio of both the monomer and macromonomer. Branches can be distributed homogeneously or heterogeneously based on the reactivity ratio of the terminal functional group on the macromonomer and the low molecular weight monomer; and, as shown in the properties section, this has a significant effect on the physical properties of the materials.

(a) **(b)**

Figure 2.20: Homogeneous distribution of grafts (a) and heterogeneous distribution of grafts (b).

The first was a single-step approach in which a methacrylate monomer (methyl methacrylate or butyl methacrylate) was copolymerized with a mixture of a PLA macromonomer and a PDMS macromonomer. The second strategy was a two-step approach in which a graft copolymer containing one macromonomer was chain-extended by a copolymerization of the second macromonomer and the low-molecular weight methacrylate monomer. The molecular structure of the terpolymers was investigated by 2D GPC which indicated that well-defined terpolymers with controlled branch distribution were prepared via both pathways. The topologies of the graft terpolymers prepared by different combinations of the two step approach.

While properties have yet to be fully explored, it is likely that phase separation is modified by polymer topology and hence the properties of the material will differ even though compositions were held constant.

2.5.2 Grafting from

In the "*grafting from*" (b) method, a polymer backbone (macroinitiator) with a predetermined number of initiation sites is generated, followed by grafting the side chains from the macroinitiator. The number of grafted chains can be controlled by the number of initiation sites generated along the backbone assuming that each one participates in the formation of one branch.

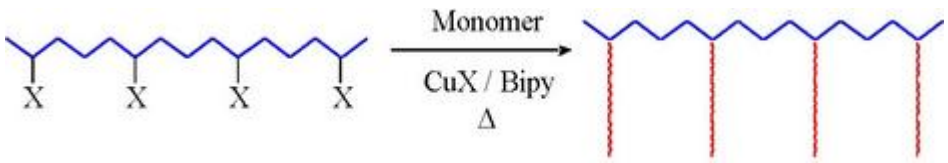

Figure 2.21 : Grafting from method.

The "*grafting from*" approach has been extensively used in the synthesis of well-defined macromolecular grafts and brushes.

C/LRP techniques are suitable for polymer brush synthesis via grafting from method since low concentration of instantaneous propagating species limit the coupling and termination reactions and the gradual growth of side chains can effectively decrease the steric effect which is inevitable for either ''*grafting-onto*'' or ''*grafting-through*'' strategies.

ATRP is a particularly attractive and has been proved to be a highly versatile method to synthesize the graft polymers with well-defined structure including the controllable molecular weight and narrow molecular weight distribution. Matyjaszewski and co-workers have previously described the controlled synthesis of molecular brush copolymers by "*grafting from*" a macroinitiator using ATRP [33].

2.5.3 Grafting onto

The ''g*rafting onto*'' method (a) relying on grafting of preformed side chains onto a backbone is carried out via a coupling reaction between the pendant functional groups distributed randomly on the backbone and the complementary end-functional groups of side chains.

The primary advantage of this method is that both backbone and side chains are prepared separately via different living polymerization techniques allowing the more accurate characterization of the resulting polymer with respect to their backbone and

side chains. On the other hand, the number of grafted polymer chains is limited due to the steric hindrance and low reactivity of functional groups of the polymer chains resulting in insufficient grafting efficiency.

Usually, ‘‘g*rafting onto*’’ reactions involve the preparation of well-defined side chains by living anionic polymerization and their subsequent reaction with a backbone of monomer units that are susceptible to nucleophilic attack. Examples of such functional groups include esters, anhydrides, benzylic halides, nitriles, chlorosilanes, and epoxides.

2.6 Photopolymerization

Photopolymerization has some advantages over thermally initiated polymerization. This is evidenced in the rapid growth of radiation curing such as curing of coating on wood, metal, and paper, adhesives, printing inks, and photoresists, which depends on the use of photoinitiators. The phenomenon of controlled radical polymerization allows for the synthesis of polymers with well-defined structures. Photoinitiators can be used in controlled radical reactions, which is also of interest. Photoinitiators are defined as being substances that have the ability to convert physical energy of an incident light beam into chemical energy, by forming reactive radical intermediates. The use of N,N-diethyl dithiocarbamate (DDC) derivatives as so-called photoiniferters during radical polymerization reactions has been reported. The term iniferter is used as first coined by Otsu, meaning substances that act as initiator, transfer agent, and terminator in radical polymerization reactions.

Photoiniferters such as DDCs and its derivatives can be used directly or as moieties attached to, inter alia, polymers. Polymeric photoiniferters have low volatility and do not suffer from initiator migration effects. Polymeric photoiniferters can also be used as precursors for block and graft polymerization reactions. Several examples of the use of DDCs in this type of application have been recently reported.The use of a combination of living cationic polymerization and radical or controlled radical polymerization to prepare block copolymers has also been reported [45].

2.7 Poly(vinyl cloride) (PVC)

Poly(vinyl chloride), better known by its abbreviation PVC, is one of the most versatile plastics. It is the second largest manufactured resin by volume worldwide

currently, its production per annum exceeds 31 milliontons. Braun described the most remarkable milestonesin PVC history, their importance to the development ofmacromolecular chemistry, and some PVC research andindustrial applications, with respect to polymerization, stabilization, bulk property modification, and chemical andmaterial recycling of PVC waste. In addition, he addressed PVC synthesis and the preparation of PVC-block-polymer by CFRP with nitroxyls.

The spectrum of PVC applications and uses is widespread and includes the following: pipes, window frames, flooring, wallpaper, window blinds, cables and wires, hoses, coatings, plastisols, packaging, medical tubingand blood bags, bottles, credit cards, audio records and imitation leather. Academic research studies on this material are numerous, starting from the remedy of its low thermal stability, which induces the dehydrochlorination process, to its chemical alteration in view of producing items for specific applications. The many organic thermal stabilizers added to PVC include N-substituted maleimides, eugenol, pyrazolones, and hydroxylbenzylthioethers. Its inferior mechanical properties have been improved by incorporating plasticizers. Also, to suppress possible deterioration within the PVC matrix, chemical stabilizers usually have been added. Recently, the addition of p-isopropenylcalixarenes in the PVC was claimed to enhance the effectiveness of lead-based stabilizers and to reduce the dehydrochlorination process. The presence of labile chlorine atoms in PVC is believed to be the dominant source of its adverse defects, giving rise to several hampering abnormalities, hence the uselessness of PVC in its virgin state. Such labile or abnormal chlorine atoms, which are mostly allylic and tertiary chlorides, are readily substituted sites, involved in manufacturing-related problems of PVC. The extensive work on modifying PVC by substituting its chlorine atoms is rather justified. A myriad of molecular and macromolecular substituents have been attached utilizing well-known and appropriate organic reactions [27]. Indeed, chemically modified PVCs have found various applications, from ion-selective electrode membranes and membrane sensors [28–29] to ion-exchange columns for metal separation [30]. Chemical modifications of PVC started more than a half-century ago and have been surveyed [27]. These modifications lie basically in the dechlorination process, including both substitution and elimination. Because of the peculiarities of the material relevant to its applications, the chemical functionalization of PVC seems permanent. Best of all was the application of the

newly developed LCRP polymerization method to the surface modification of PVC and other polymers [30].

The graft copolymers of PVC with BA and EHA were synthesized by using ATRP and this synthesis was showed below (Figure 2.22). This study was realized by Niyazi Bicak and Mesut Ozlem. They used PVC as macroinitiator, n-butyl acrylate and 2 ethyl hexyl acrylate as monomer. CuBr was used as catalyst and H-TETA was used as ligand. The reaction was carried out under nitrogen, 1,2-dichlorobenzene was used as solvent and reaction was occured at 90°C. The polymerization was continued for 7.5 hours.

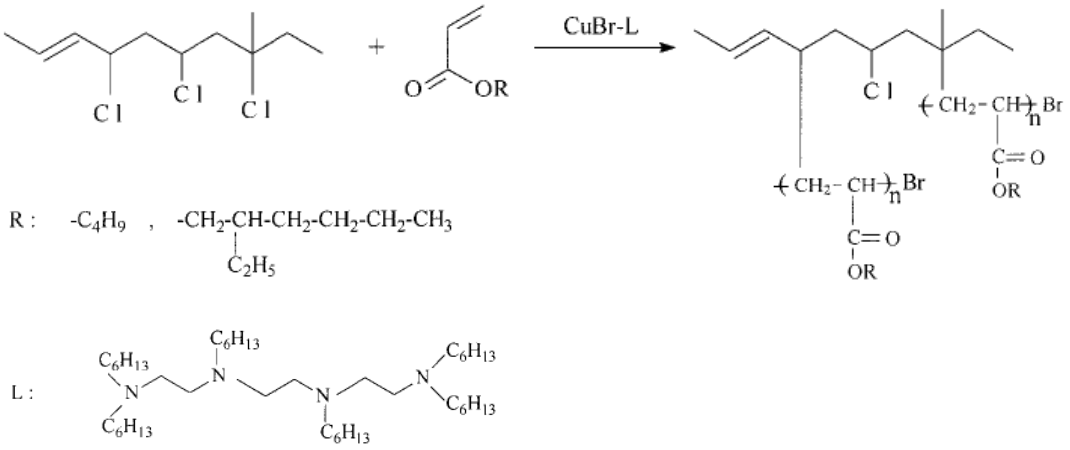

Figure 2.22 : Grafting of acrylate monomers from labile chlorines of PVC.

This reaction was characterized by using ^{1}H-NMR and GPC. They found that The grafting of PVC at 90 °C was reasonably fast for both monomers. Grafting yields of 161.8 and 51.2% were attained in 7.5 h for BA and EHA monomers [31].

Table 2.1 : Graft copolymerization characteristics of BA and EHA from PVC.

Monomer	Initial Concentration (M)[a]	[M]/[Cu-L][b]	Graft Yield (%)[c]	First-Order Rate Constant	$M_n \times 10^{-3}$	PDI[d]
BA	1	100/1	161.8	3.34×10^{-5} s^{-1}	130	1.64
EHA	1	100/1	51.2	4.48×10^{-6} s^{-1}	106	1.56

[a] In 1,2-dichlorobenzene at 90 ± 1 °C.
[b] Molar ratio of the monomer to the copper complex.
[c] Calculated from the mass increase for a reaction time of 7.5 h.
[d] For the graft copolymer.

Polymerization of AMPS via ATRP have some problem, so, generally, poymerization of AMPS is carried out with using AMPS sodium salt. As showed below (Figure 2.23), PAMPS was achieved with ATRP and, for this reaction, sodium 2-acrylamido-2-methylpropanesulfonate was used as monomer, 2-chloropropionate

as initiator, CuCl /$CuCl_2$/tris(2-dimethylaminoethyl)amine (Me_6TREN) as catalytic system [32]. This reaction was realized in DMF.

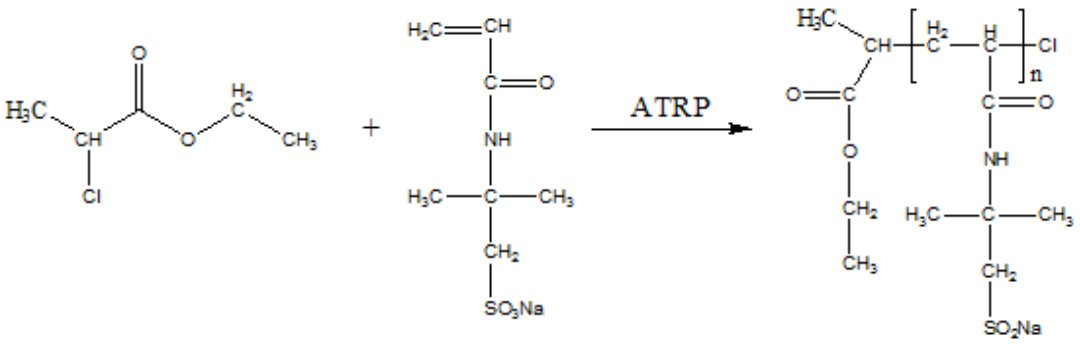

Figure 2. 23 : Polymerization of AMPS via ATRP.

Reaction was characterized by using ^{1}H-NMR, GPC, HPLC, fluorescence measurements, dynamic light scattering (DLS) and energy filtered-transmission electron microscopy (EF-TEM).

The *N,N*-diethyldithiocarbamate group was UV-sensitive. Small molecular compounds containing *N,N*-diethyldithiocarbamate groups had the properties of bioactivity, accelerating the crosslinking of rubber and initiating the polymerization of vinyl monomers under UV irradiation or heating. By introducing the *N,N*-diethyldithiocarbamate groups into polymer chain, the functional polymer thus obtained not only had the properties of the group itself but also provided the way for further modification of the polymer. Jianjun Guan and Wenjun Yang was synthesized Poly(vinyl chloride) (PVC) with pendent *N,N*-diethyldithiocarbamate and was reported. The reaction was characterized by using UV-Visible spectrophotometer and FT-IR insturments [46].

Khalifa Al-Kaafi and Albert J. Van Reenen was synthesized Poly(epichlorohydrin) (PECH) with pendent N,N-diethyl dithiocarbamate groups (PECH-DDC) and than this DDC pendent groups were used for photopolymerization via iniferter polymerization technique [47]. The synthesis mechanism was shown in Figure 2.24 and 2.25.

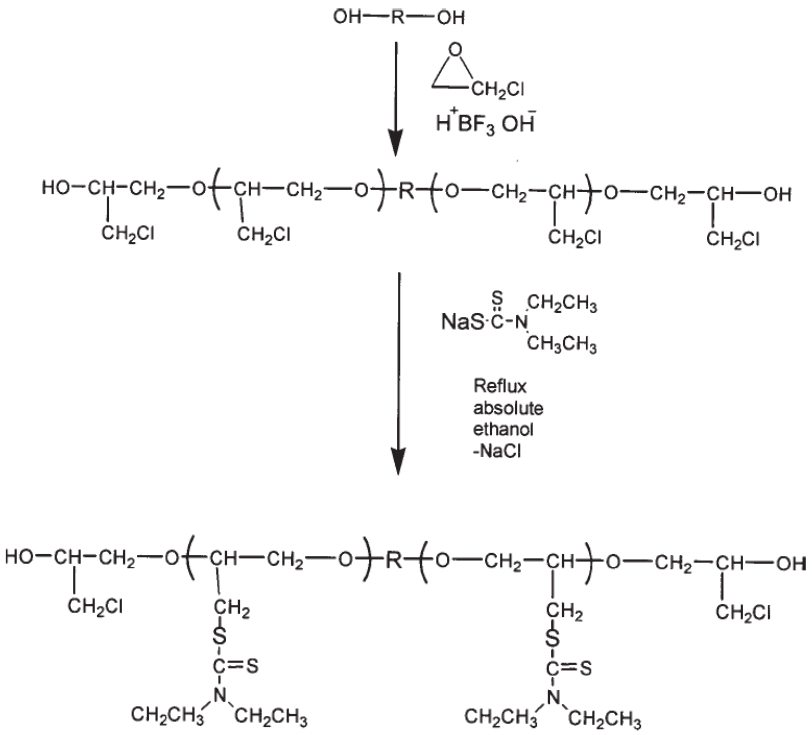

Figure 2.24: Synthesis of Poly(epichlorohydrin) (PECH) with pendent N,N-diethyl dithiocarbamate groups (PECH-DDC).

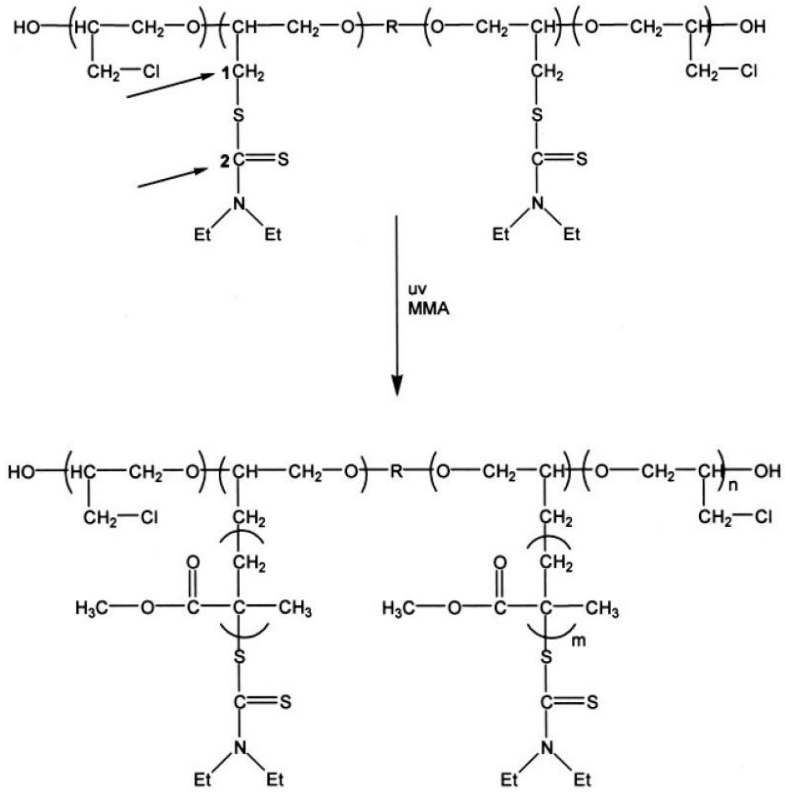

Figure 2.25: Synthesis of PECH-g-PMMA via iniferter polymerization.

3. EXPERIMENTAL PART

3.1 Chemicals

Poly(vinyl chloride) was purchased from Akay Plastik San. Tic. A.Ş. 2-Acrylamido-2-methylpropan sulfonic acid (AMPS, Figure 3.1) was purchased from Lubrizol. *N*,*N*,*N*',*N*'',*N*''-Pentamethyldiethylenetriamine (PMDETA, 99 %) was purchased from Merck. Copper (I) bromide (CuBr 98%) and diethyldithiocarbomic acid sodium salt trihydrate (Figure 3.2) were purchased from Across Organics Co. Tetrahydrofuran (THF 99.9%) and N,N-dimethylformamide (DMF 99.8 %) were purchased from Labkim. N-Methyl-2-pyrrolidone (NMP, 99.5 %) and ethyl methyl ketone (MEK 99.0 %) were purchased from Sigma – Aldrich. Dichloromethane (technical purity), chloroform (99.5 %) was purchased from Carlo Erba, methanol (MeOH (technical purity)) and diethyl ether was purchased from Honeywell.

Table 3.1 presents the chemical structures of homopolymer PVC that has a moleculer weight of 84K (molecular weight of PVC was measured by triple detector GPC, light scattering, IR and viscometer) and Nafion® which is commercial polymer electrolyte membrane for fuel cells. Figure 3.1 presents the monomer that is used to synthesise graft copolymers of PVC by ATRP.

Table 3.1 : Chemical structures of PVC and Nafion®-117

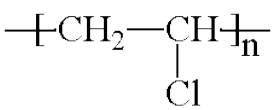 PVC 84K	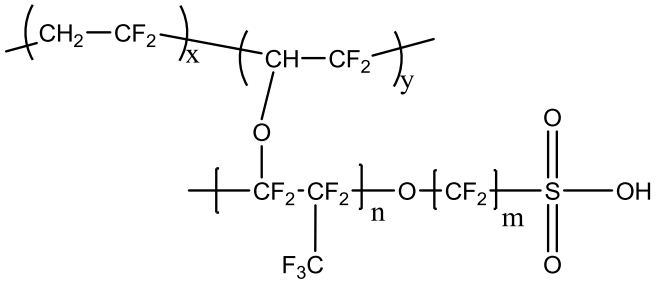 Nafion®(Nafion117)

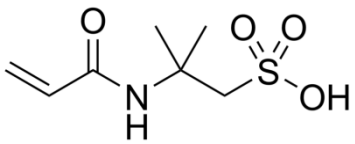

Figure 3.1 : 2-Acrylamido-2-methylpropan sulfonic acid (AMPS)

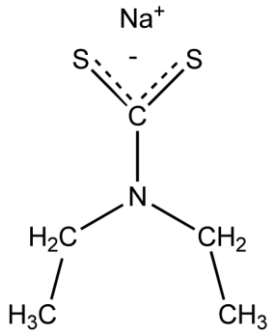

Figure 3.2: Sodium diethyldithiocarbomate used as iniferter precursor.

3.2 Synthesis of P(VC-*g*-AMPS) Graft Copolymer by ATRP

In order to synthesis of P(VC-*g*-AMPS), PVC (0.5 g, 8 x 10^{-3} eq mol repeating unit), which is used as macroinitiator, was dissolved in 6 mL of DMF and the solution was stirred through 40 minutes at 50 ^{o}C. Meanwhile, AMPS (0.3316 g, 1.6 x 10^{-3} eq mol (20 % of repeating unit of PVC), which is used as monomer, was dissolved in 2 mL of DMF. The solution was stirred through 15 minutes at room temperature.

Then, ATRP procedure was performed as follows; CuBr (0.023 g, 1.6 x 10^{-4} mol) as catalyst was placed in a 48 mL of flask, which contained a side arm with a Teflon valve sealed with a Teflon stopper. Then the flask was deoxygenated by 3 circles of vacuum-nitrogen-vacumm. PVC solution, AMPS solution and PMDETA (0.033 mL, 1.6 x 10^{-4} mol) as ligand priory nitrogen bubbled were added to the flask, respectively. Then mixture was nitrogen bubbled 15 minutes before the flask was replaced in thermostatically controlled oil bath at 90 °C with 500 rpm stirring rate to initiate the graft copolymerization. The reaction was maintained 48 hours. To control the polymerization, alequot was taken via syringe from the reaction solution. Samples were precipitated in methanol and filtered. After filtration, polymer samples were dried for 24 h in a vacuum oven at 50 ^{o}C.

Finally, P(VC-*g*-AMPS) graft copolymers were further purified by desired time in an excess amount of water at room temperature to remove the unreacted AMPS monomer. In addition, after purification, the samples was dissolved in THF and

passed through alumina column in order to remove the residual copper from the polymer solution, if any. Then, the solution were reprecipitated in methanol, filtered and dried for 24 h in a vacuum oven at 50 ^{o}C.

3.3 Synthesis of PVC-DDC (diethyl dithiocarbomate)

PVC–DDC was synthesized from the reaction of PVC with sodium diethyl dithiocarbomate trihydrate. PVC (3 g), butanone (180 mL), and sodium diethyl dithiocarbomate trihydrate (2.16 g, %20 of PVC repeating unit) were placed in a 500-mL, flask equipped with a motor stirrer, a reflux condenser and a temperature controller. The reaction was continued under stirring for 6 h at 60°C. The solution was then poured into a large amount of methanol. The precipitated products were purified by reprecipitating from the butanone–methanol system and dried under vacuum.

3.4 Synthesis of P(VC-*g*-AMPS) Graft Copolymer by Iniferter Polymerization

In order to synthesis of P(VC-*g*-AMPS), PVC-DDC (0.1 g, 3.2 x 10^{-4} eq mol repeating SR unit) was dissolved in 8 mL of DMF and the solution was stirred through 20 minutes at room temperature. Meanwhile, AMPS (0.0633g , 3.2 x 10^{-4} mol), which is used as monomer, was dissolved in 2 mL of DMF. The solution was stirred through 5 minutes at room temperature.

PVC-DDC macrophotoinitiator solution and AMPS solution were placed into the photoreactor tube. The tube was nitrogen bubbled throughout 20 minutes before the tube was replaced in photoreactor at 25 ^{o}C. The reaction was maintained 1.5 hours at 280 nm. Samples were precipitated in methanol and filtered. After filtration, polymer samples were dried for 24 h in a vacuum oven at 50 ^{o}C.

Finally, P(VC-*g*-AMPS) graft copolymers were further purified by desired time in an excess amount of water at room temperature to remove the residual AMPS monomer.

3.5 Characterization Methods

3.5.1 Infrared spectrometer (FT-IR)

FT-IR spectra were recorded on a Thermo Nicolet 6700 FT-IR spectrometer.

3.5.2 UV-Visible spectrophotometer

UV – Visible spectra were recorded on a Shimadzu UV – 1601 UV – visible spectrophotometer.

3.5.3 Gel permeation chramatography (GPC)

The conventional Gel Permeation Chromatography (GPC, Figure 3.3) measurements were conducted in THF at 30 °C using an Agilent instrument (Model 1100) consisting of a pump (0.3 mL/min) and four Waters Styragel columns (guard, HR 5E, HR 4E, HR 3, HR 2), (4.6 mm internal diameter, 300 mm length) in series with two detection systems: a refractive index and UV detectors). BHT was used as an internal standard. The determination of apparent molecular weights for the polymers was based on linear PS standards (Polymer Laboratories).

Figure 3.3: Gel permeation chromatography.

The second GPC system is equipped with an Agilent model isocratic pump, guard and four Waters Styragel columns (guard, HR 5E, HR 4, HR 3, and HR 2), and a Viscotek TDA 302 triple detector (RI, dual laser light scattering (LS) (λ= 670 nm, 90° and 7°) and a differential pressure viscometer). TD-GPC (Figure 3.4) was conducted to measure the absolute molecular weights in THF with a flow rate of 0.5 mL/min at 35 °C. All three detectors were calibrated with a PS standard having narrow molecular weight distribution (M_n= 115,000 g/mol, M_w/M_n= 1.02, [η]= 0.519 dL/g at 35 °C in THF, d*n*/dc= 0.185 mL/g) provided by Viscotek company. Typical sample concentrations for GPC-analysis were in the range of 1–10 mg/mL depending

on molecular weight of analyzed polymers. Data analyses were performed with OmniSec 4.5 software from Viscotek Company.

Figure 3.4: Triple detector GPC.

3.5.4 Differential scanning calorimetry (DSC)

Differential scanning calorimetry (DSC, Figure 3.5) measurements were done to find out glass transition temperature (T_g) values using TA instruments Q1000 series. To avoid the influence of the thermal history, thermograms were evaluated from the first heating run in a range of 0 to 200 °C with 10 °C.min^{-1} ramp rate. Cooling ramp is not specified and equilibrate command was used. Then, the thermograms were evaluated from the second heating run in range of 0 to 270 ^{o}C with 10 ^{o}C.min^{-1} ramp rate . All tests were carried out under 50 ml.min^{-1} rate of nitrogen purge. All T_g measurement were investigated on TA Universal Analysis software by the inflection of change in the endothermic direction of the heating ramp.

Figure 3.5 Differential scanning calorimetry (DSC, TA Q1000).

3.5.5 Electrochemical impedance spectroscopy (EIS)

Electrochemical impedance spectroscopic (Figure 3.6) measurements were conducted at room temperature (25 ^{o}C) using the conventional three electrode cell configuration. The electrochemical cell was connected to a potentiostat (Parstat 2263-1), which interfaced to a computer. An electrochemical impedance software (Powersine) was used to carry out impedance measurements by scanning in the 10 - 100 kHz frequency range with applied AC signal amplitude of 10 mV. The impedance spectra were analyzed using AC impedance data analysis software (ZSimpWin V3.10).

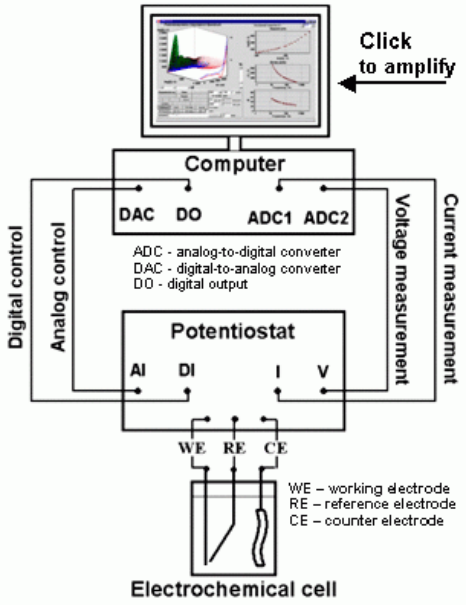

Figure 3.6 General diagram of electrochemical impedance spectroscopy.

3.5.6 Nuclear magnetic resonance spectroscopy (NMR)

^{1}H NMR measurements (Figure 3.7) were recorded in d_7-DMF and d_6-DMSO, using an Agilent VNMRS500 (500 MHz) instrument.

Figure 3.7 : Agilent VNMRS500 NMR insturment.

3.5.7 Thermal gravimetric analysis (TGA)

TGA measurements were recorded by using TA-Q50 TGA instrument (Figure 3.8). The tests were carried out 20 ^{o}C/min ramp rate.

Figure 3.8 : TA-Q50 TGA instrument.

4. RESULTS AND DISCUSSION

4.1. PVC-Based Graft Copolymer

For the synthesized of PVC-based proton exchange membrane, AMPS monomer, which can transport H^+ with $-SO_3H$ groups, was grafted to PVC backbone via ATRP and iniferter methods. Some preliminary results were shown in Table 1. Amount of AMPS monomer was used as 20 % of repeating unit of PVC backbone for each method. After the synthesis of P(VC-*g*-AMPS), its characterizations and proton transportation properties were investigated .

Table 4.1 Previous experiments.

Syntheses	Used Materials	Target	Problem
PCP-DDC	Poly(chloroprene) and Sodium dithiocarbomate	Hydrolisis of DDC group thiol group (-SH) for Thiol-Ene reaction	Solubility problems, precipitation problems and complex structure
PVC-DDC	Poly(vinyl chloride) and Sodium Diethyl Dithiocarbomate	Hydrolisis of DDC group to compose thiol group (-SH) for Thiol-Ene reaction and also use as iniferter agent	
Model Compound	Hexylbromide and Sodium dithiocarbomate	To find molar absorption coefficient of DDC and to determine dithiocarbomate group content in PVC	Co-Solvent problem with PVC-DDC
PVC-SH	PVC-DDC and Triethylamine	Hydrolisis of DDC group to thiol group (-SH) for Thiol-Ene reaction	Reaction didn’t achieve

PVC-SH	PVC-DDC and Hexylamine	Hydrolisis of DDC group to thiol group (-SH) for Thiol-Ene reaction	Reaction didn't achieve
PVC-SH	PVC-DDC and Ethylenediamine	Hydrolisis of DDC group to thiol group (-SH) for Thiol-Ene reaction	Reaction didn't achieve

4.1.1. P(VC-*g*-AMPS) graft copolymer via ATRP

PVC as macroinitiator and AMPS (0.2 eq mol to PVC) as monomer was used in the graft polymerization by using ATRP method. Synthesis reaction of graft copolymer via ATRP method is shown in Figure 4.1.

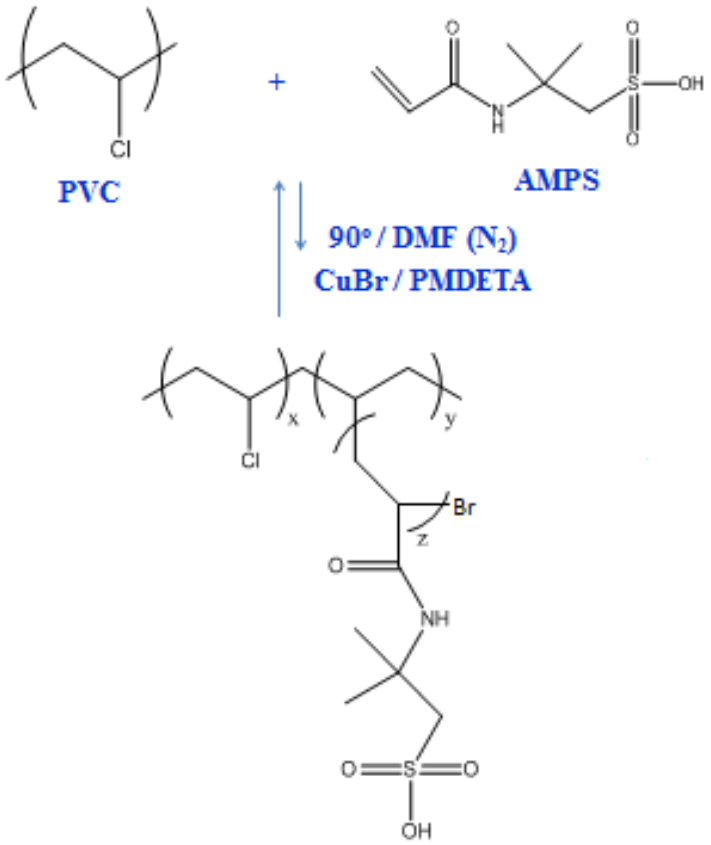

Figure 4.1: Synthesis of P(VC-*g*-AMPS) copolymer via ATRP method.

Three samples were taken from the polimerization solution for 5, 24 and 48 hours in order to monitor the grafting yields.

As described previously, polymerization of AMPS via ATRP method has some problems. So, , polymerization of AMPS generally carry out with preparing sodium salt of AMPS monomer. Grafting reaction was realized without preparing sodium

salt of AMPS monomer. So, UV results were firstly evaluated to see whether the grafting polymerization occurs or not.

As can be seen from Figure 4.2, UV absorbance of graft copolymer increases by time because of addiction of AMPS monomer. After 5 hours, a little increase in absorbance is seen and after 24 hours, UV absorbance peak also increases up to two times. After 48 hours, UV absorbance peak is almost equall with 24 hours.

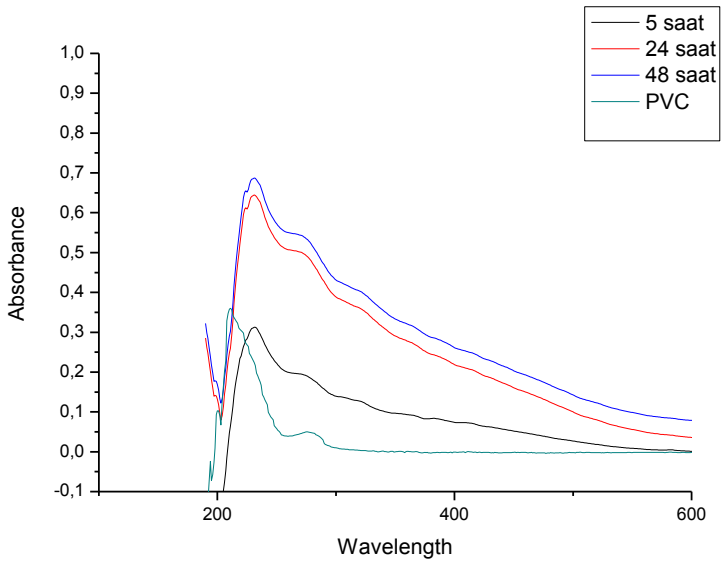

Figure 4.2: UV-Visible spectra of P(VC-*g*-AMPS) [P(VC-*g*-AMPS)]= 0.66mg/mL.

IR spectra of P(VC-*g*-AMPS), AMPS monomer and PVC are represented in Figure 4.3 and Figure 4.4.

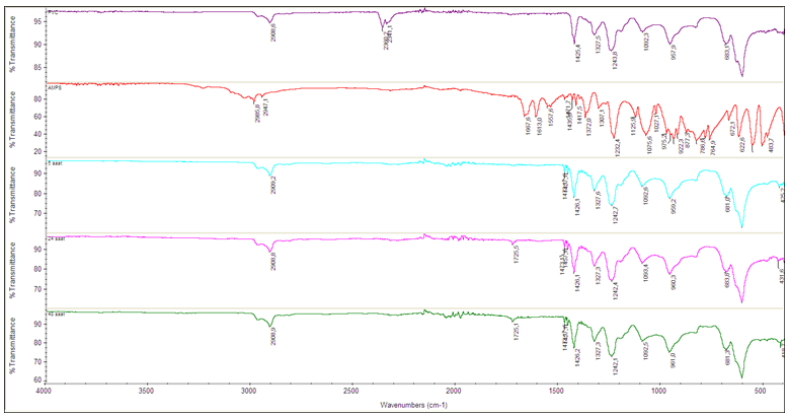

Figure 4.3: IR spectrum of AMPS monomer, PVC and the samples of P(VC-*g*-AMPS) at 5, 24 and 48 hours.

It can be seen that in Figure 4.3, C=C double bond conjugated with C=O at 1613 cm^{-1} and C=O conjugated with C=C double bond at 1667 cm^{-1} for AMPS monomer.

Whereas, a new peak at 1725 cm^{-1} in 3 spectra of P(VC-*g*-AMPS) for 5, 24 and 48 hours, belonging to only the carbonyl group C=O, is clearly shows that the AMPS monomer was polymerized, i.e. conjugation was disappeared.

As can be seen in Figure 4.4, while no any absorption peak was observed between 1600 cm^{-1} and 1750 cm^{-1} for PVC, a new absorption peak is slightly appeared at 1725 cm^{-1} for graft copolymer in 5 hrs and is increased by time, can be concluded that AMPS content is increased in the graft copolymers.

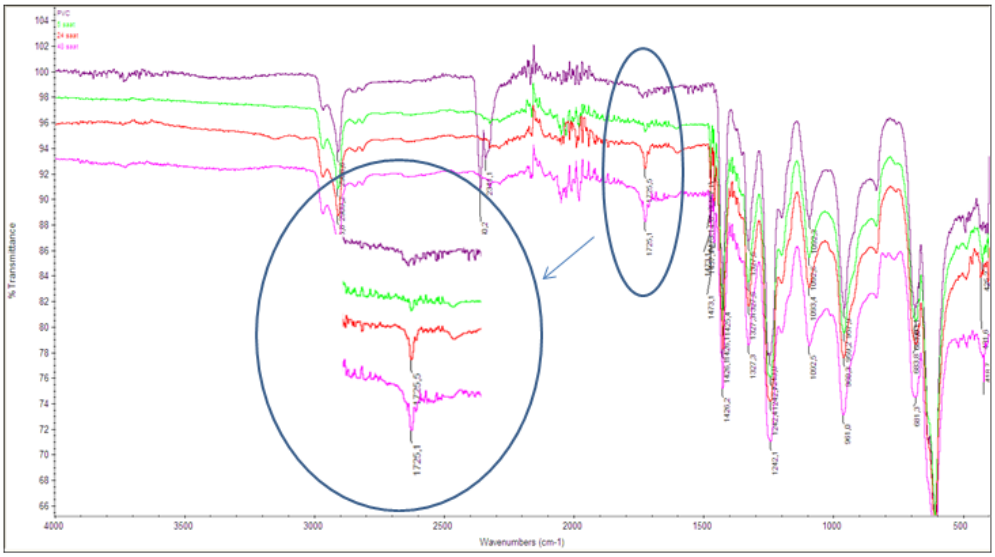

Figure 4.4: IR spectrum of PVC and P(VC-*g*-AMPS) at 5, 24 and 48 hours.

(T_g) is very important for polymeric materials, hence it is a function of chain flexibility. The glass transition occurs when there is enough vibrational (thermal) energy in the system to create sufficient free-volume to permit sequences of 6-10 main-chain carbons to move together as a unit. At this point, the mechanical behavior of the polymer changes from rigid and brittle to tough and leathery. This behavior, we define as "plastic behavior".

After FT-IR and UV-Visible results, termal behavior of P(VC-g-AMPS) was investigated by using differantial scanning calorimetry in order to see T_g value of the obtained materials.

For first heating cycle (Figure 4.5) of DSC measurement, P(VC-*g*-AMPS) samples 5, 24 and 48 hours were heated from 0 to 230 ^oC. After first heating cycle, materials were cooled to 0 ^{o} C. For second heating cycle (Figure 4.6), samples were heated again from to 270 ^oC.

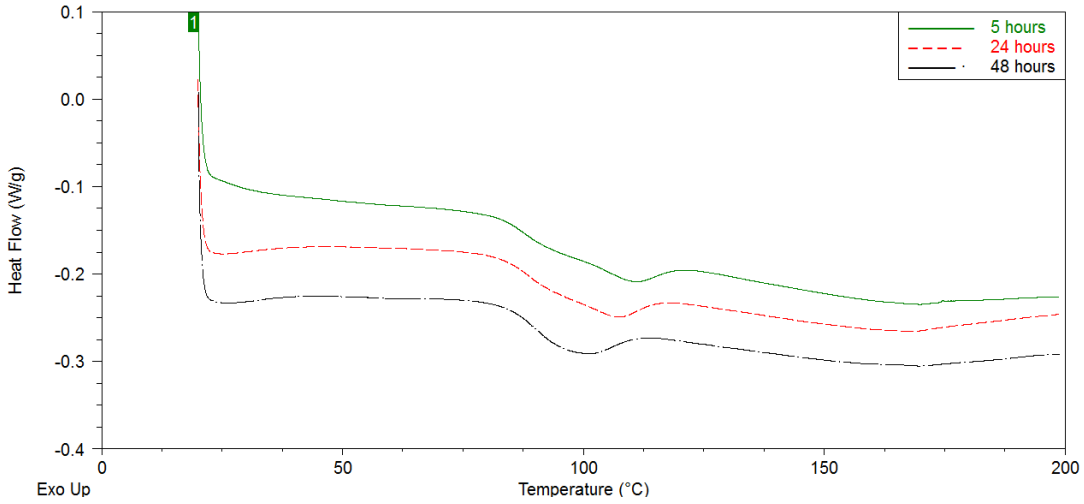

Figure 4.5: DSC curves of P(VC-*g*-AMPS) at 5,24 and 48 hours (first heating cycle).

Since the melting point of AMPS monomer is 195 ^{o}C and any melting point can not be seen in the DSC curves (Figure 4.5), it can be concluded there is no any residue of AMPS monomer in the powder polymeric metarial.

The first cycle of DSC curves were used only in order to see whether there is any residue of monomer in the polymer. Generally, first cycle of DSC curve generally use in order to remove humidity or other contaminants and erase thermal history from the polymeric materials. Therefore, to find the T_g values of the (co)polymers, the second cycle of DSC curves were used (Figure 4.6).

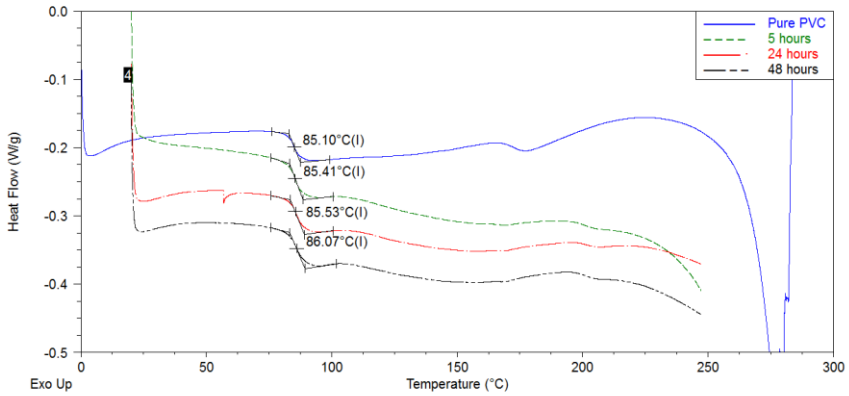

Figure 4.6: DSC curves of PVC and P(VC-*g*-AMPS) at 5,24 and 48 hours (second heating cycle).

As can be seen from the DSC curve of PVC, its T_g value is 85.10 ^{o}C and the grafting polymerization progresses, T_g values were slightly increased.

Table 4.2: T_g values of pure PVC and P(VC-*g*-AMPS) samples.

Sample	T_g (^oC)
PVC	85.10
P(VC-*g*-AMPS) 5 hours	85.41
P(VC-*g*-AMPS) 24 hours	85.53
P(VC-*g*-AMPS) 48 hours	86.07

GPC separates the abundance and chain length of polymer based on the size or hydrodynamic volume (radius of gyration) of the analytes. This differs from other separation techniques which depend upon chemical or physical interactions to separate analytes. Separation occurs via the use of porous beads packed in a column.

The smaller analytes can enter the pores more easily and therefore spend more time in these pores, increasing their retention time. Conversely, larger analytes spend little if any time in the pores and are eluted quickly. All columns have a range of molecular weights that can be separated.

Conventional GPC results (Figure 4.7) of graft copolymer P(VC-*g*-AMPS) were investigated in order to see M_n and PDI values of the samples and the results are represented in Table 4.2. The results were calculated by GPC software (WinGPC) according to PS calibration.

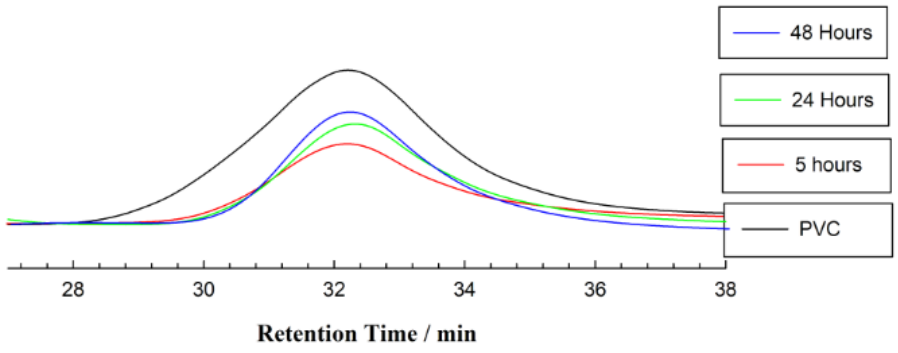

Figure 4.7: The conventional gel permeation chromatography (GPC) measurements of PVC and P(VC-*g*-AMPS) at 5,24 and 48 hours.

Table 4.3 : M_n and PDI values of the samples.

Samples	M_n (g/mol)	PDI
PVC	100,520	3.94
P(VC-*g*-AMPS) 5 hours	102,550	2.24
P(VC-*g*-AMPS) 24 hours	88,470	2.19
P(VC-*g*-AMPS) 48 hours	86,750	1.92

As can be seen Table 4.3, M_n and PDI values were decreased by the polymerization time. Normally, while the grafting is increasing, molecular weight of the polymer also increase. However, according to the Table 4.2, while the grafting is increasing, molecular weight of the polymer decrease. This circumstance can be explained by random coil and decreasing of hydrodynamic volumes of the graft copolymer samples. As can be seen structure of AMPS, due to its -OH groups it can make hydrogen bonds with each other while amount of grafting AMPS monomer increases. These hydrogen bonds might cause decreasing of the hydrodynamic volume of the polymer samples in RI detector therefore decreasing of the molecular weight.

At the fifth hours of the grafting polymerization, the molecular weight of the sample increases a little from 100,520 g/mol to 102,550 g/mol. After 24 hours, the molecular weight decreases from 102,550 g/mol to 88,470 g/mol. For 48 hours, the molecular weight is almost same (86,750 g/mol) with 24 hours sample.

Triple detection sets has become the preferred method for characterizing natural and synthetic polymers. It employs a concentration detector, viscometer and light scattering detector acting in concert, with each detector providing complementary but different information. The light scattering detector provides a direct measurement of absolute molecular weight and eliminates the need for column calibration. The viscometer detector provides a direct measurement of intrinsic viscosity or molecular density, and allows the determination of molecular size, conformation and structure. Concentration is measured with an RI or UV, and is necessary for the determination of both molecular weight and intrinsic viscosity.

Triple detection has a unique advantage in that it provides absolute molecular weight, molecular size (to less than 1 nm) and intrinsic viscosity, as well as information on conformation, branching.

Triple detection is able to accomplish all this - and more - without the need for lengthy column calibration.

Unlike the conventional GPC, in order to give aabsolute moleculer weight of polymers, when triple detection GPC was used, where it can be expected an increase in the molecular weight of the samples by time. The samples were measured by using triple detection GPC and the results are represented in Figure 4.8. M_n, PDI and R_h values of the samples are represent in Table 4.4.

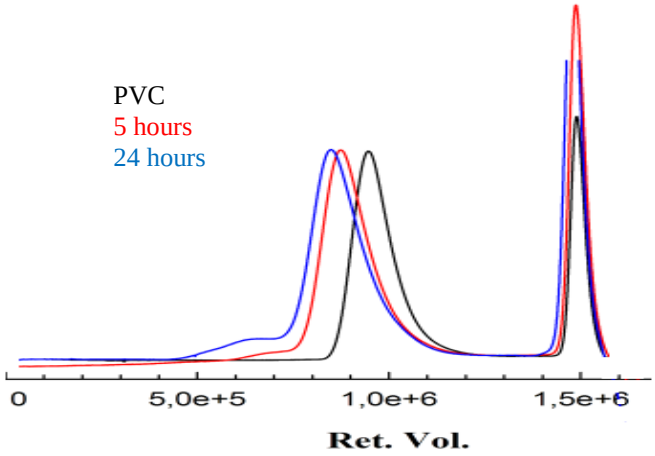

Figure 4.8: Triple detection GPC results of PVC and P(VC-*g*-AMPS) at 5 and24.

Table 4.4 : M_n, PDI and R_h value of the samples by GPC-TD.

Sample	M_n (g/mol)	PDI	R_h
PVC	84,195	1.72	11.02
P(VC-*g*-AMPS) 5 hours	129,472	1.71	11.94
P(VC-*g*-AMPS) 24 hours	160,121	1.39	12.77

As can be seen from Table 4.4, molecular weight of the samples increases the grafting time. While, the absolute molecular weight of the pure PVC is 84,000 g/mol, after the 5 hours of the grafting, moleculer weight increases from 84,195 to 129,472 g/mol and after 24 hours, molecular weight attain 160,121 g/mol. In addition to increase the molecular weight, R_h value of the samples were also increased from 11.02 to 12.77. The PDI values was also decreased from 1.72 to 1.71 for pure PVC and P(VC-*g*-AMPS) at 5 hours, , PDI value was decreased to 1.39 at 24 hours.

The main target of this study is to synthesis an ion conductive polymer. After characterization of P(VC-*g*-AMPS) by using FT-IR, UV-Visible spectrophotometre, DSC and GPC, ion conductivity of the P(VC-*g*-AMPS) by using Electrochemical

Impedance Spectroscopy (EIS) was investigated. After the Electrochemical Impedance Spectroscopy measurements, nyquist graph (Figure 4.9) and magnetude graph (Figure 4.10) were obtained:. The samples were prepared in DMF as solvent, 0.3g sample was dissolved in 12.5 ml DMF.

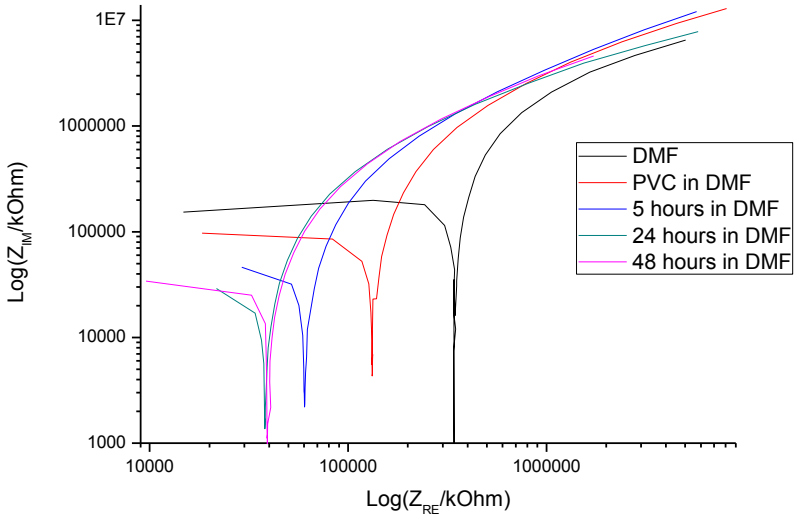

Figure 4.9: Nyquist graph of EIS measurements.

X scale of the nyquist graph shows the resistance of the solution. Where, it can be clearly seen that DMF has maximum resistance. the resistance decreases more than pure PVC For P(VC-*g*-AMPS) at 5 hours and the resistance of P(VC-*g*-AMPS) at 24 hours and 48 hours less than the others and they are almost same. According to these results P(VC-*g*-AMPS) was shown ion conductivity.

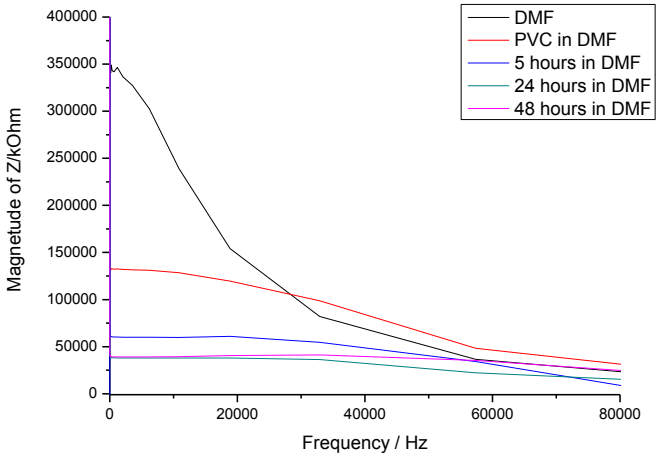

Figure 4.10: Magnetude graph of EIS measurements.

In contrast to the nyquist graph, y scale of the magnitude graph shows the resistance and according to Figure 4.10, it can be seen that DMF has maximum resisdance and P(VC-*g*-AMPS) sample at 24 and 48 hours have minimum resistance. Just as nyquist graph, these results also show the graft copolymers have ion conductivity.

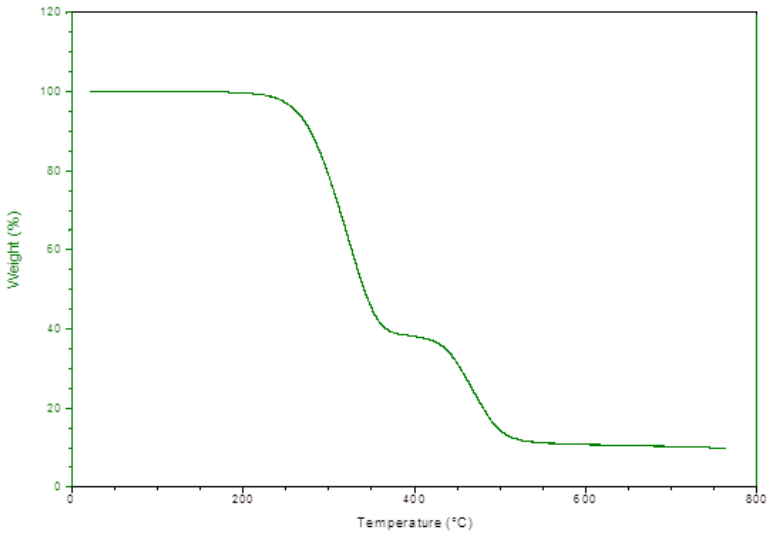

Figure 4.11 : TGA result of P(VC-*g*-AMPS) via ATRP.

As can be seen Figure 4.10, PVC decomposition begins at 260 ^{o}C due to HCl elimination and other decomposition of PVC and AMPS group begin at 390 ^{o}C.

4.1.2. Synthesis of PVC-DDC

The precursor of PVC graft AMPS copolymer, PVC-DDC was synthesized by the reaction of PVC and sodium diethyl dithiocarbamate according the Figure 4.12.

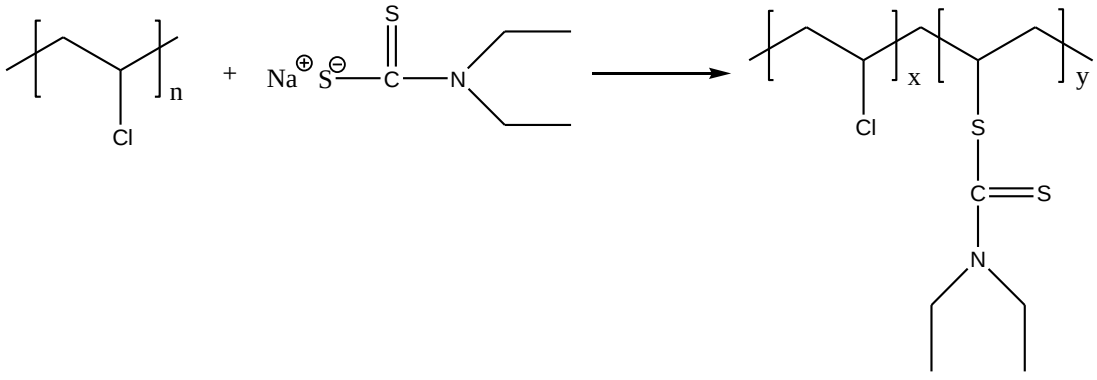

Figure 4.12 : The synthesis route of PVC-DDC.

The successful synthesis of PVC-DDC was confirmed by FT-IR (Figure 4.13), UV-Visible spectrophotometer (Figure 4.14) and ^{1}H NMR (Figure 4.15). There were

facts that could show the occurrence of the substitution reaction of PVC with DDC. Sodium chloride was precipitated during the reaction. The weight of product increased after the reaction, owing to the change of substitution amount on the PVC side chain.

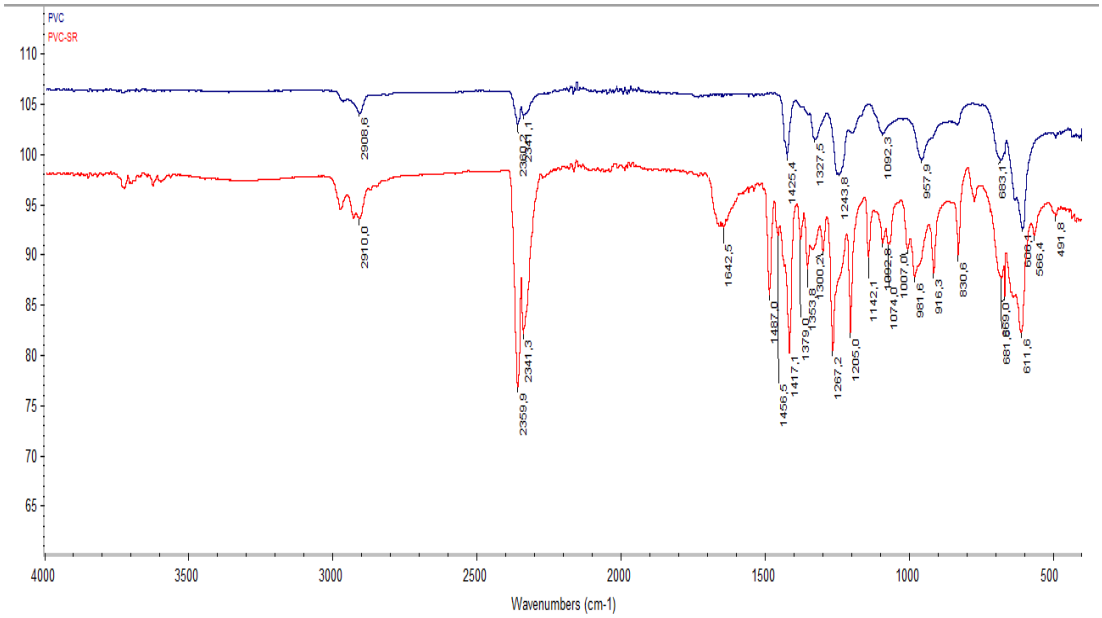

Figure 4.13 : IR spectrum of PVC and PVC-DDC.

The FTIR spectra of PVC and PVC with DDC pendant groups were compared and characteristic peaks due to the –SC(S)N and –C(=S)-N groups appearing at 916, 981, 1417 cm^{-1} and 1204, 1266, 1487 cm^{-1} could be assigned. An newpeak at1642 $cm^{-1}$is appeared in the IR spectrum of PVC–DDC which is important characteristic peak of -SC(S)N.

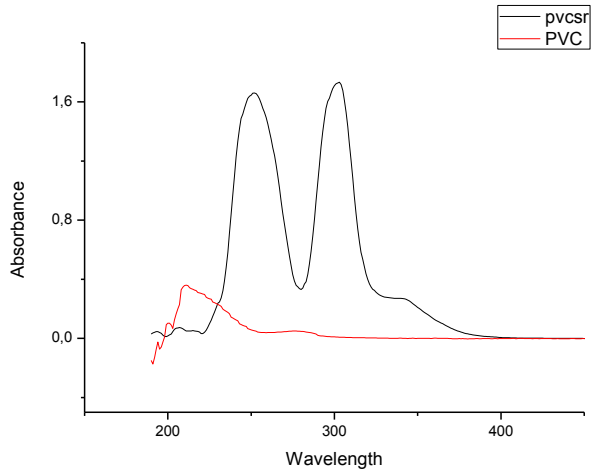

Figure 4.14 : UV spectrum of PVC and PVC-DDC.

The ultraviolet absorption spectra of PVC and PVC-DDC are shown in Figure 4.14. The conjugated absorbent peaks for –S-C=S at 251 nm and S=C-N at 302 nm areappeared in the UV spectrum of PVC–DDC. THF was used as solvent and concentration of the samples is 0.001 g/mL.

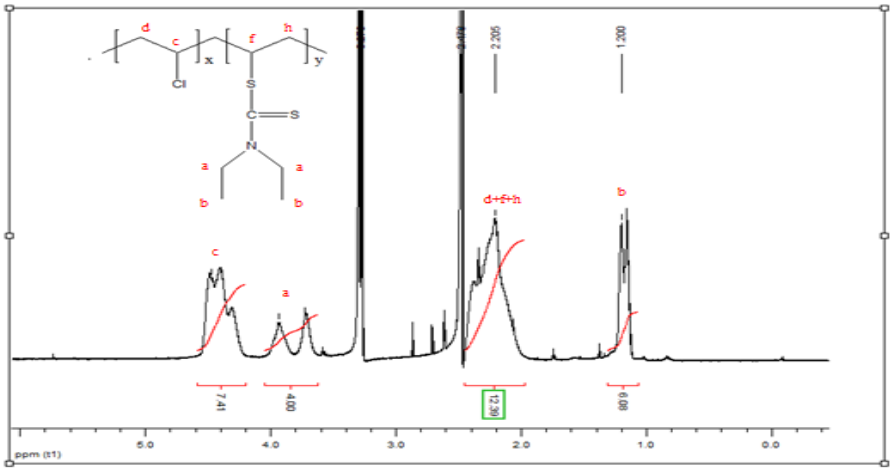

Figure 4.15 : ^{1}H NMR spectrum of PVC-DDC.

As can be seen from Figure 4.15, six hydrogens of -CH_3 group (b) of DDC are appeared at 1.12 ppm and four hydrogens of –N(CH_2) group (a) of DDC are appeared between3.97-3.81 ppm .

Calculation of x and y values was represented in equation 4.1 (integrated value of c proton that belonging -CH-Cl group in PVC backbone compared to the integrated value of a protons).

x/7.41=4y/4 ; x=7.41y & x+y=1 ; y=1/8.14=0.12 , x=0.88 **(4.1)**

4.1.3. P(VC-*g*-AMPS) via iniferter method

Synthesis reaction of graft copolymer via iniferter method is shown in Figure 4.16.

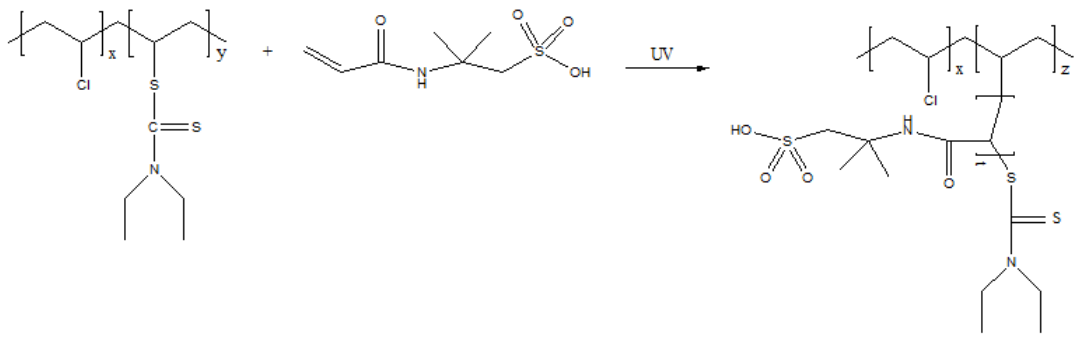

Figure 4.16 : Synthesis of P(VC-*g*-AMPS) via iniferter method.

Synthesis of P(VC-g-AMPS) graft copolymer via iniferter method using PVC-DDC_2 (Table 4.6) was confirmed by FT-IR (Figure 4.17), DSC (Figure 4.18), (H^1 NMR (Figure 4.19) and UV-VIS (Figure 4.20).

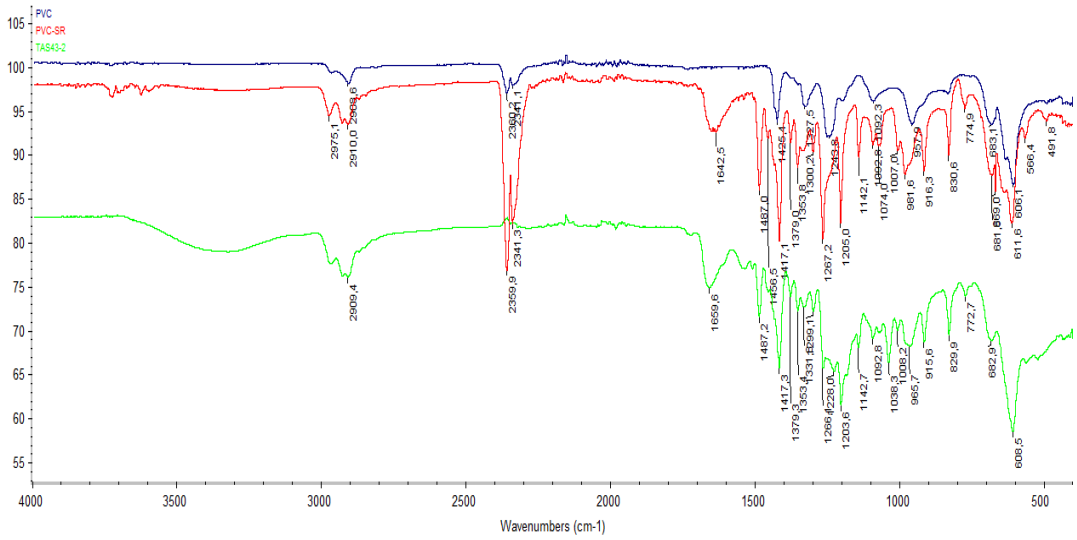

Figure 4.17 : FT-IR result of P(VC-*g*-AMPS) by iniferter method.

As can be seen from Figure 4.17, there is a broad peak at 3300 cm^{-1}. This peak references to the –OH group of AMPS monomer. The peak of -SC(S)N group at 1642 cm^{-1} shifts to 1660 cm^{-1} due to the C=O group in AMPS monomer. In addition to this peaks, the new peaks are appeared at 965, 1038, 1228, 1331 cm^{-1}.

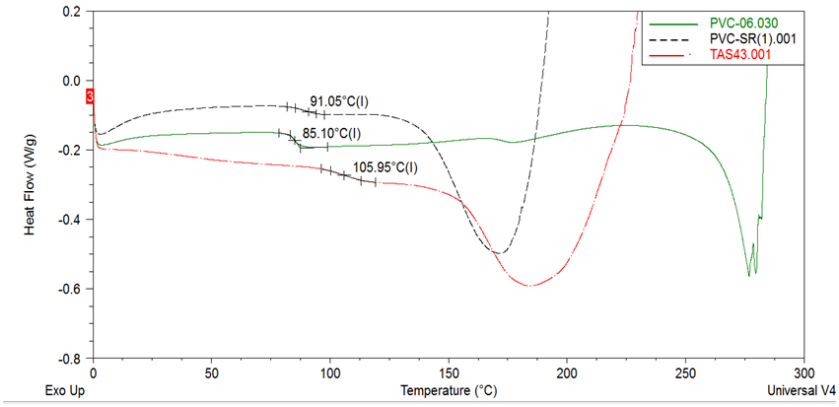

Figure 4.18 : DSC result of P(VC-*g*-AMPS) by iniferter method.

Thermal behavior and differences of P(VC-*g*-AMPS) samples were investigated by using DSC insturement. As can be seen from Figure 4.18, T_g value of PVC is 85 ^oC, PVC-DDC is 91.5 ^oC and when the grafting polymerization progress, T_g value of P(VC-*g*-AMPS) increases to 105.95 ^oC. These results are show that the grafting was progresses and thermal resistance of the sample was increased.

Table 4.5 : T_g values of PVC, PVC-DDC and P(VC-*g*-AMPS).

Sample	T_g (^oC)
PVC	85.10
PVC-DDC	91.50
P(VC-*g*-AMPS)	105.95

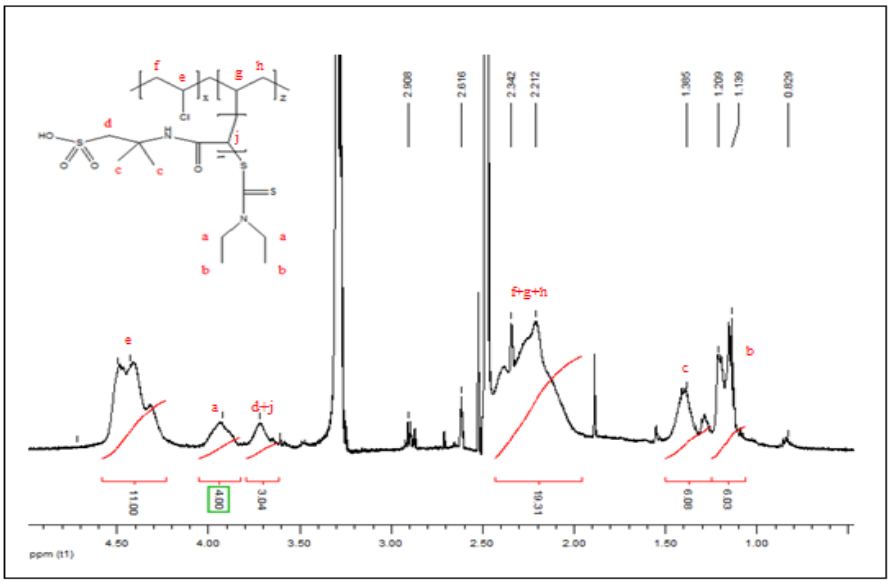

Figure 4.19 : ^{1}H-NMR of P(VC-*g*-AMPS) by iniferter method.

As can be seen from Figure 4.19, six hydrogens of -CH_3 group (b) of DDC are appeared at 1.12 and four hydrogens of –N(CH_2) group (a) of DDC are appeared at3.9 ppm. A hydrogen of –CH(C=O) group (j) and two hydrogen of –CH_2(SO_3H) (d) group of AMPS are appeared at 3.7 ppm. Six hydrogens of -NH-C(CH_3)$_2$ group (c) of AMPS are also appeared at 1.3 ppm. Broad peaks as called (e) and (f+g+h) refer to hydrogens of PVC backbone.

Calculation of x and z values was represented in equation 4.2 (integrated value of e proton that belonging -CH-Cl group in PVC backbone compared to the integrated value of a protons).

x/11=4z/4 ; x=11y & x+z=1 ; z=1/12=0.08 , x=0.92 **(4.2)**

Calculation of l value was represented in equation 4.3 (integrated value of c protons of AMPS monomer compared to integrated value of a protons of DDC group);

4(a protons)L/4 = 6(c protons)/6 ; L=1 **(4.3)**

Calculation of $M_{n,P(VC\text{-}g\text{-}AMPS)}$;

$M_{n,GPC(LS)}$ of PVC: 84000 g/mol ; $M_{A,VC}$: 62.5g/mole ; 84000/62.5 g/mol=1344 rep. unit. 1344x8/100=108 rep.unit of DDC group, 108x((207.25+148.26+27) =~41310 g/mol;

1344x92/100=1236 rep.unit of VC group, 1236x62.5=77280 g/mol.

$M_{n,P(VC\text{-}g\text{-}AMPS)}$=77280+41310=118590 g/mol.

Table 4.6 : DDC group content of PVC-DDC.

Syntheses	DDC group content[a]	Usage
PVC-DDC_1	12%	Used in characterization
PVC-DDC_2	8%	Used as iniferter macroinitiator

a : Calculated by ^{1}H NMR

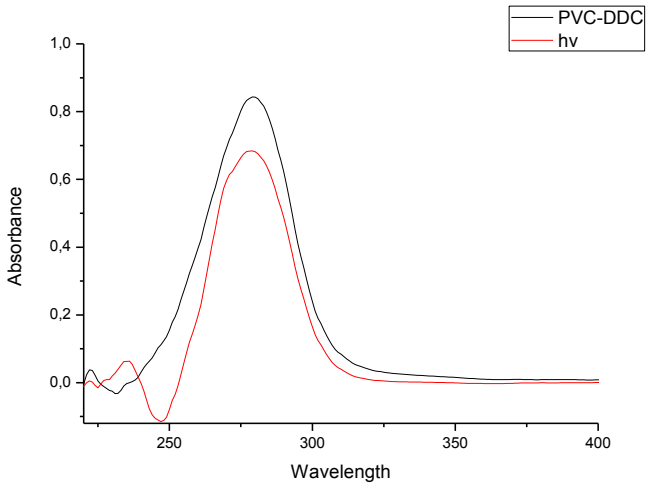

Figure 4.20 : UV-Visible Spectrophotometer results of PVC-DDC_2 and P(VC-*g*-AMPS) graft copolymer via iniferter method.

As can be seen UV-Visible results of P(VC-*g*-AMPS) via ATRP (Figure 4.20), UV absorbance peak of AMPS grafted monomer is at 234 nm. According to figure 4.20, for P(VC-*g*-AMPS) via iniferter method (red line), same UV absorbance peak of AMPS grafted monomer is seen at same place (234 nm). UV absorbance peak of DDC group is seen 278 nm and absorbance peak of DDC group decreases after reaction. Since the same concentration was used for each sample, the decreasing of absorbance peak of DDC group can be concluded that the amount of DDC group decreases by the graft copolymerization.

Termal decomposition of the graft copolymer was investigated by TGA instruments and represented in Figure 4.21.

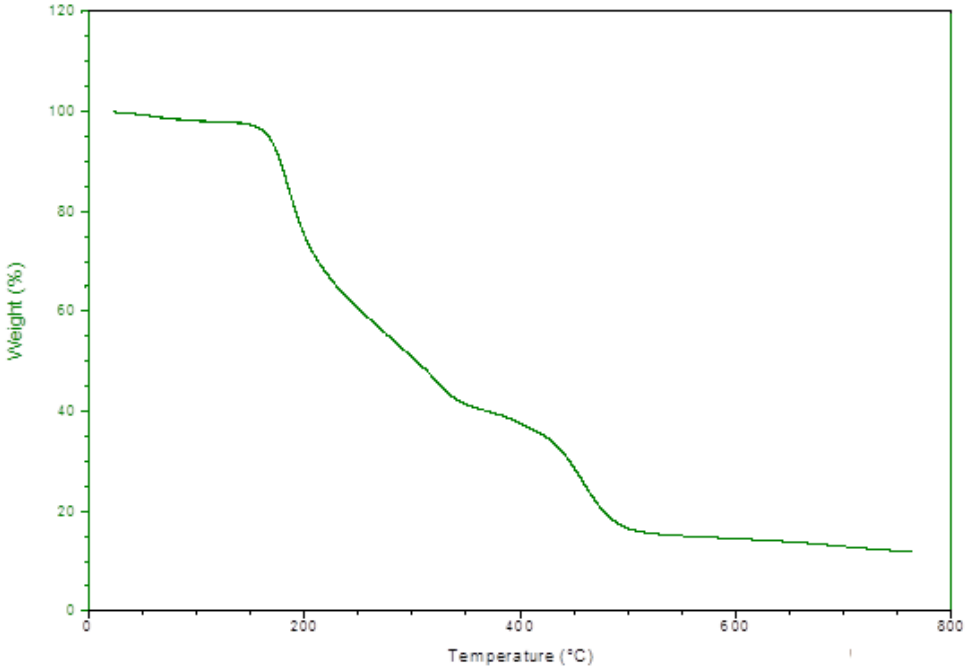

Figure 4.21 : TGA result of P(VC-*g*-AMPS) graft copolymer via iniferter method.

As can be seen Figure 4.21, termal decomposition of graft copolymer begins at 190 ^{o}C because of DDC groups. Then, typical PVC decomposition begins at 260 ^{o}C due to HCl group elimination on PVC backbone and other decomposition of PVC and AMPS group begin at 390 ^{o}C.

P(VC-*g*-AMPS) graft copolymer wer obtained by ATRP and iniferter methods are shown some differences in T_g values and dissolution properties. These differences can be different amount of AMPS monomer in each P(VC-*g*-AMPS) samples. Addition of AMPS monomer to PVC by iniferter method is more than addition by ATRP method that can be seen elugram shift in from conventional GPC (solvent: DMF) (Figure 4.22 and 4.23).

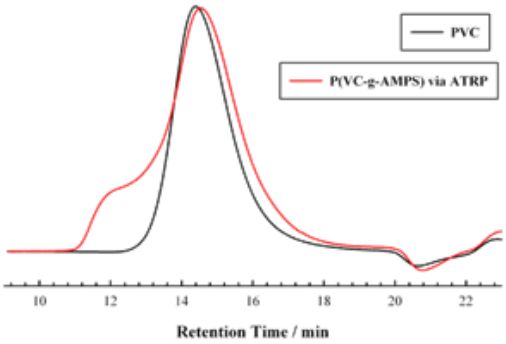

Figure 4.22 : DMF GPC results of PVC and P(VC-*g*-AMPS) by ATRP method.

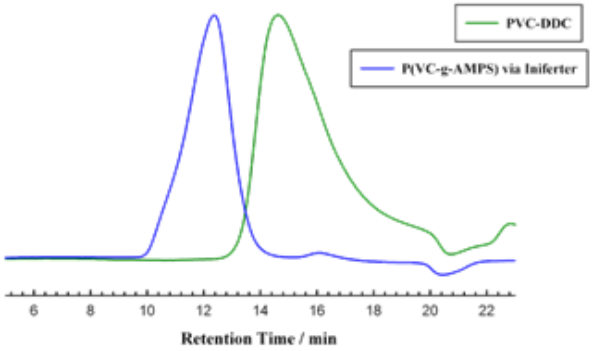

Figure 4.23 : DMF GPC results of PVC-DDC and P(VC-*g*-AMPS) by iniferter

As can be seen nyquist graph of EIS (Figure 4.24), although concentration of reactants at iniferter method were less than the concentration of reactants at ATRP method, P(VC-*g*-AMPS) via iniferter method has more ion conductivity (less resistance) than P(VC-*g*-AMPS) via ATRP method. From these results, it can be concluded the addition amount of the monomer in iniferter method more than in ATRP method.

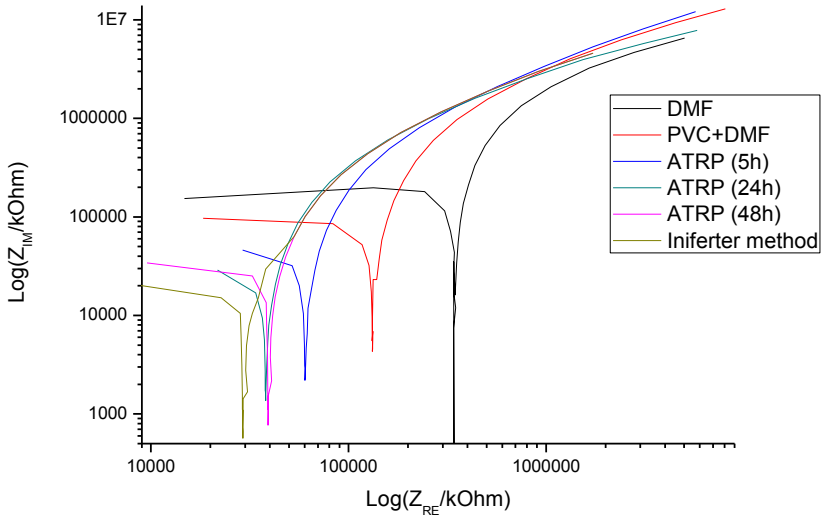

Figure 4.24 : Nyquist graph of EIS measurements for ATRP and iniferter method.

5. CONCLUSION

In the development of new proton exchange membranes (PEM) for fuel cells, functionalization of a polymer offers many advantages, in particular with respect to the mechanical properties and the price of the material. Functionalization is possible with graft or block copolymerization.

The first aim of this study was to develop alternative membranes that have suitable thermal and chemical stability, comparable proton conductivity and relatively low cost. In this respect, PVC based graft copolymers with AMPS monomer were synthesized by using two different graft copolymerization methods.

Firstly, P(VC-*g*-AMPS) was synthesized by using ATRP method. Polymerization of AMPS via ATRP have some problem. So, poymerization of AMPS is generally carried out with using AMPS sodium salt. In this study, grafting copolymerization of AMPS monomer was achieved without preparing AMPS sodium salt. The synthesis of graft copolymerization of AMPS was demonstrated by using different characterization instruments such as FT-IR, UV-Visible spectrophotometer, conventional and triple detector GPC. Thermal properties of PVC based copolymer were investigated by using DSC measurements and a little increase of T_g value of the material was observed. Termal decomposition of PVC based copolymer was investigated by using TGA instrument and was found termal decomposition stages.

The main aim of this study was to synthesize ion conductive polymer. So, after synthesize and characterize of P(VC-*g*-AMPS), ion conductivity of the material was investigated by using electrochemical impedance spectroscopy (EIS). Increase of ion conductivity of P(VC-*g*-AMPS) was demostrated by using the nyquist and magnetude results of EIS spectroscopy.

After synthesize of P(VC-*g*-AMPS) by using ATRP method, PVC based copolymer was synthesized by using another polymerization method, iniferter polymerization method. For synthesize of P(VC-*g*-AMPS) by iniferter method, sodium diethyl dithiocarbomate group was used as iniferter. So, PVC containing *N*,*N*-diethyl dithiocarbomate group to be 20% of repeating unit of PVC was synthesized.

Obtained PVC-DDC was characterized by using UV-Visible spectrophotometer, FT-IR and ^{1}H NMR instruments.

Then, PVC-DDC polymer was used as macrophotoinitiator in order to synthesized P(VC-*g*-AMPS) via iniferter polymerization method and obtained graft copolymer was characterized by using FT-IR and ^{1}H NMR. Side chain amount is calculated as one from ^{1}H NMR spectrum for PVC-*g*-AMPS. Thermal behavior of the material was inventigated by using DSC. A significant increase in the T_g value of PVC-*g*-AMPS was observed when it compared with synthesis of PVC-*g*-AMPS via ATRP method. Termal decomposition of PVC based copolymer via iniferter method was investigated by using TGA instrument and was found termal decomposition stages.

After synthesized of each polymer, they were put in 100 ^{o}C water and stirred throughout two hours. The end of two hours, dissolution wasn't observed for each samples.

Different thermal and dissolution properties were observed for two graft copolymers (PVC-*g*-AMPS) that were obtained by two different methods (ATRP and iniferter methods).

PVC-*g*-AMPS via iniferter method is shown more ion conductivity (less resistance) than P(VC-*g*-AMPS) via ATRP method. Next step of this study can be to prepare of PVC-*g*-AMPS films and to compare with conventional fuel cell membranes in terms of advantages and disadvantages.

REFERENCES

[1] **Pimentel, D. and Pimentel, M. H.,** (2008). Food, Energy and Society, *Renewable Energy:Current and Potential Issues,* Taylor & Francis Group, Boca Raton, London, New York.

[2] **Vasquez, L. O.,** (2007). Fuel Cell Research Trends, Nova Science, New York.

[3] **Twidell, J. and Weir, T.,** (2006). Renewable Energy Resources, Taylor & Francis Group, New York.

[4] **Url-1** <*http://www.renewableenergyworld.com/rea/tech/hydrogen/*>, date retrieved 15.10.2012.

[5] **Sorrell, C. S., Sugihara, S. and Nowotny, J.,** (2005). Materials for Energy Conversion Devices, *Polymer Electrolyte Fuel Cells,* Woodhead and Maney, Boca Raton, Boston, New York, Washington DC.

[6] **Thomas, G. J. and Jones, R. H., (**2008). Materials for the Hydrogen Economy, *Materials for Proton Exchange Membrane Fuel Cells,* Taylor & Francis Group, Boca Raton, London, New York.

[7] "*ACC Resin Statistics Annual Summary*". date retrieved 18.11.2012.

[8] **Url-2 <** *http://www.jt-extrudermachine.com/pvc_polyvinyl_chloride_sheet.htm*>, date retrieved 15.10.2012.

[9] **Aggour, Y. A.,** (1994). Thermal degradation of copolymers of 2-acrylamido-2-methylpropane sulphonic acid with acrylamide. *Polymer Degradation and Stability*, 44, 71.

[10] **Sauguet, L., Boyer, C., Ameduri, B. and Boutevin, B.,** (2006). Synthesis and characterization of poly(acrylic acid)-graft-poly(styrene) graft copolymers obtained by atom transfer radical polymerization of styrene. *Macromolecules,* 39, 9087-9101.

[11] **Manahan, S. E.,** (2001). Fundamentals of Environmental Chemistry, *Chemistry and Electricity* , LLC, Boca Raton.

[12] **Wheeler, D. and Sverdrup, G.,** 2007:2008 Status of Manufacturing: Polymer Electrolyte Membrane (PEM) Fuel Cells.

[13] **Shipp, D. A.,** (2005). Living radical polymerization: Controlling molecular size and chemical functionality in vinyl polymers. *Journal of Macromolecular Science-Polymer Reviews,* 45 (2), 171-194.

[14] **Tunca, U., Hizal, G., Acar, MH., Tasdelen, MA., Yagci, Y., Mishra, MK**., *''Handbook of Vinyl Polymers: Radical Polymerization and Technology''*

[15] **Url-3 <** *http://www.cmu.edu/maty/about-atrp.html* >, date retrieved 16.10.2012.

[16] **Matyjaszewski, K. and Xia, J.,** (2001). Atom Transfer Radical Polymerization. *Chem. Rev.*, 101, 2921-2990.

[17] **Wang, J. S. and Matyjaszewski, K.,** (1995). Controlled/Living Radical Polymerization. Halogen Atom Transfer Radical Polymerization Promoted by a Cu(I)/Cu(II) Redox Process. *Macromolecules,* 28, 7901-7910.

[18] **Patten, T. E. and Matyjaszewski, K.,** (1998). Atom transfer radical polymerization and the synthesis of polymeric materials. *Adv. Mater.,* 10, 901-915.

[19] **Shipp, D. A. and Matyjaszewski, K.,** (2000). Kinetic analysis of controlled/"living" radical polymerizations by simulations. 2. apparent external orders of reactants in atom transfer radical polymerization. *Macromolecules,* 33, 1553–1559.

[20] **Matyjaszewski, K., Patten, T. E. and Xia, J.,** (1997). Controlled/Living Radical Polymerization-Kinetics of the Homogeneous Atom Transfer Radical Polymerization of Styrene. *J. Am. Chem. Soc.,* 119, 674-680.

[21] **Davis, K., Paik, H. J. and Matyjaszewski, K.,** (1999). Kinetic investigation of the atom transfer radical polymerization of methyl acrylate, *Macromolecules* 32, 1767-1776.

[22] **Wang, J. L., Grimaud, T. and Matyjaszewski, K.,** (1997). Kinetic Study of the Homogeneous Atom Transfer Radical Polymerization of Methyl Methacrylate. *Macromolecules,* 30, 6507–6512.

[23] **Percec, V., Barboiu, B. and Kim, H. J.,** (1998), Arenesulfonyl halides: A Universal Class of Functional Initiators for Metal-Catalyzed "Living" Radical Polymerization of Styrene(s), Methacrylates, and Acrylates. *J. Am. Chem. Soc.,* 120(2), 305–316.

[24] **Percec, V., Barboiu, B., Neumann, A., Ronda, J. C. and Zhao, M.,** (1996). Metal-catalyzed "living" Radical Polymerization of Styrene Initiated.

[25] **Koh, J. H., Kim, Y. W., Park, J. T. and Kim, J. H.,** (2008). Templated Synthesis of Silver Nanoparticles in Amphiphilic Poly(vinylidene fluoride-co-chlorotrifluoroethylene) Comb Copolymer. *Journal of Polymer Science: Part B: Polymer Physics,* 46, 702–709.

[26] **Kamigaito, M., Ando, T. and Sawamoto, M.,** (2001). Metal-Catalyzed Living Radical Polymerization. *Chem. Rev.,* 101, 3689-3745.

[27] **Moulay, S.,** (2010). Chemical Modification of poly(vinylchloride). *Progress in Polymer Science,* 35, 303–331

[28] **Cosofret, V.V., Lindner, E., Buck, R. P., Kusy, R. P., Whitley, J. Q**., (1993). Electrochemical characterization of aminated PVC-based ion-selectivemembranes. *Electroanalysis*, 5, 725–30.

[29] **Shishkanova, T. V., Volf, R., Krondak, M., Král, V,.** (2007). Functionalization of PVCmembrane with ss oligonucleotides for a potentiometric biosensor. *Biosens Bioelectron*, 22, 2712–7.

[30] **Liu, P.,** (2007), Modification of Polymeric Materials via Surfaceinitiated Controlled/“Living” Radical Polymerization. *e-Polymers*, 62, 1–30.

[31] **Biçak, N., Ozlem, M.,** (2003). Graft Copolymerization of Butyl Acrylate and 2-Ethyl Hexyl Acrylate from Labile Chlorines of Poly(vinyl chloride) by Atom Transfer Radical Polymerization. *Journal of Polymer Science: Part A: Polymer Chemistry*, Vol. 41, 3457–3462.

[32] **Masci, G., Diociaiuti, M., Crescenzi, V**., (2008). ATRP Synthesis and Association Properties of Thermoresponsive Anionic Block Copolymers. *Journal of Polymer Science: Part A: Polymer Chemistry*, Vol. 46, 4830–4842

[33] **Beers, K.L., Gaynor, S.G., Matyjaszewski, K., Sheiko, S.S., and Moller, M.**, (1998). The Synthesis of Densely Grafted Copolymers by Atom Transfer Radical Polymerization. *Macromolecules*, 31, 9413-9415.

[34] **Szwarc M., L.M., and Milkovich R.,** (1956). Polymerization Initiated by Electron Transfer to Monomer. A New Method of Formation of Block Polymers. *J. Am. Chem. Soc.*, 78, 2656-2657.

[35] **Szwarc, M.**, (1956). Living Polymers. *Nature*, 178, 1168-1169.

[36] **Miyamoto, M., Sawamoto, M., and Higashimura, T.,** (1984). Living Polymerization of Isobutyl Vinyl Ether with the Hydrogen Iodide Iodine Initiating System. *Macromolecules*, 17, 265-268.

[37] **Tasdelen, M. A., Kahveci, M. U., Yagci, Y.,** (2011). Telechelic Polymers by Living and Controlled/Living Polymerization methods, *Progresss in Polymer Science*, 36(4), 455-567.

[38] **Chiefari, J., Chong, Y.K., Ercole, F., Krstina, J., Jeffery, J., Le, T.P.T., Mayadunne, R.T.A., Meijs, G.F., Moad, C.L., Moad, G., Rizzardo, E., and Thang, S.H.**, (1998). Living Free-Radical Polymerization by Reversible Addition-Fragmentation Chain Transfer: The RAFT Process. *Macromolecules*, 31, 5559-5562.

[39] **Barner-Kowollik, C.,** (2008). *Handbook of Raft Polymerization*, Weinheim: Wiley-VCH.

[40] **Moad, G., Rizzardo, E., and Thang, S. H.**, (2006), Living Radical Polymerization by the RAFT Process. *Aust. J. Chem.*, 59, 669-692.

[41] **Moad, G., Rizzardo, E., and Thang, S. H.**, (2009). Living Radical Polymerization by the RAFT Process. *Aust. J. Chem.*, 62, 1402-1472.

[42] **Moad, G., Rizzardo, E., and Thang, S. H.**, (2008). Toward Living Radical Polymerization. *Acc. Chem. Res.*, 41, 1133-1142.

[43] **Moad, G., Chiefari, J., Chong, Y. K., Krstina, J., Mayadunne, R. T. A., Postma, A., Rizzardo, E., and Thang, S. H.**, (2000). Living Free Radical Polymerization with Reversible Addition-Fragmentation Chain Transfer (the Life of Raft). *Polym. Int.*, 49, 993-1001.

[44] **Alberti, A., Benaglia, M., Laus, M., Macciantelli, D., and Sparnacci, K.**, (2003). Direct ESR Detection of Free Radicals in the RAFT Polymerization of Styren., *Macromolecules*, 36, 736-740.

[45] **Al-Kaabi, K., Van Reene, A. J.,** (2008). Controlled Radical Polymerization of poly(methylmethacrylate-g-epichlorohydrin) Using N,N ditihiocarbomate-mediated Iniferters. *Journal of Applied Polymer Science*, 108, 2528–2534.

[46] **Guan, J., Yang, W.,** (2000). Photografting of PVC containing *N,N* diethyldithiocarbomate groups with vinyl monomers. *Journal of Applied Polymer Science*, **77**, 2569–2574.

[47] **Al-Kaabi, K., van Reenen, A.J.**, (2008). Controlled radical polymerization of poly(methyl methacrylate-*g*-epichlorohydrin) using *N,N*-dithiocarbamate-mediated iniferters. *Journal of Applied Polymer Science*, 108, 2528–2534

[48]**Url-4** < *http://www.fuelcelltoday.com/about-fuel-cells/benefits* >, date retrieved 13.12.2012.

[49] **Otsu, T., Kuriyama, A.,** (1985). Polymer design by iniferter technique in radical polymerization. *Polymer J.*, 17, 97.

CURRICULUM VITAE

Name Surname: Cüneyt Erdinç TAŞ

Place and Date of Birth: Istanbul / 11.04.1985

Address: ITÜ Personal Lojmanları, A-12 Blok D:11. Maslak / İstanbul

E-Mail: c.e.tas@hotmail.com

B.Sc.: Chemist / Zonguldak Bülent Ecevit University

Professional Experience and Rewards:

Professional Experience,

- Researcher ; KOSGEB / M-POL Company , 2010 -
- Organizing committe member ; International Controlled/Living Polymerization Symposium, 2011, Antalya,Turkey (Co-Chairmens: Prof. Metin H. Acar and Prof. Krzysztof Matyjaszewski)
- Organizing committe member ; XXIV. National Chemistry Symposium, 2010, Zonguldak, Turkey (Chairmen: Prof. Baki Hazer)
- Internship ; ITU Chemical & Metallurgical Engineering Faculty, Prof. Dr. Nusret Bulutçu Research Laboratory (03/07/ 2008 – 05/08/2008).
- Internship ; ITU Faculty of Science and Letters, Prof. Dr. Metin H. Acar Research Laboratory (10/08/2009 – 07/09/2009)

Rewards,

- Zonguldak Bülent Ecevit University Faculty of Science and Latters certificate of achievement (2007 and 2010) (because of academic degree)
- Zonguldak Bülent Ecevit University Faculty of Science and Latters Sporting Achievement Certificate (2008) (as player of Faculty Voleyball Team)
- Zonguldak Bülent Ecevit University Certificate of Appreciation (Because of social activities in Cinema Student Committe)

PUBLICATIONS/PRESENTATIONS ON THE THESIS

- Acar, M.A., **Tas, C.E**., Proton exchange membranes fuel cell design via Atom Transfer Radical Polimerization. *IV. National Polymer Science and Technology Symposium*, September 5-8, 2012 Çanakkale, Turkey.